Refined Hydro-environmental Modelling for Tidal Energy Generation: West Somerset Lagoon Case Study

Bin Guo, Reza Ahmadian*, Roger A Falconer

School of Engineering, Cardiff University, The Parade, Cardiff CF24 3AQ, U.K.

Corresponding author: Reza Ahmadian, Queens Building, Cardiff University, 5 The Parade, Roath, Cardiff, U.K. CF24 3AA. Email: AhmadianR@cardiff.ac.uk

Abstract

An accurate assessment of the hydro-environmental impacts of tidal range energy schemes, where the performance of the scheme has an impact on the marine environment and ecology, is crucial in optimising the design and development of such schemes. A proposal for a new coastally-attached impoundment, namely West Somerset Lagoon, has been investigated in this research study and the numerical model TELEMAC-2D has been refined to model the impacts of this scheme on the Bristol Channel and Severn Estuary. Domain decomposition was applied and full momentum conservation between the subdomains was included in the model by implementing momentum source terms at the turbine locations. The results have confirmed the importance of including full momentum conservation in modelling the effects of turbo-machinery in tidal lagoons. It was found that the operation of the scheme decreased the high water level slightly in the Bristol Channel and Severn Estuary, while there was a decrease in the low intertidal areas. The maximum velocity and bed shear stress were predicted to increase in the inner Bristol Channel, while they decreased noticeably across most of the interior of the lagoon, away from the turbine wakes. Furthermore, the operation of the lagoon significantly improved the water renewal in the region.

Keywords: Tidal Lagoons; Hydrodynamic Modelling; Environmental Impact Assessment; Lagoon Operation; Momentum Conservation

1 Introduction

Marine renewable energy has been widely considered in many countries with potentially vast marine resources [1-4]. One of the oldest forms of marine renewable energy is tidal range energy. A Tidal Range Scheme (TRS) is capable of generating predictable energy from tides by utilizing an artificial water head difference, generated by impounding water throughout a tidal cycle. Tidal lagoons, which generally do not block major estuaries to the same extent as barrages, have tended to have reduced impacts on the estuarine environment and ecology, as well as potentially offering many of the multifunctional features of barrages, such as flood risk reduction, etc [5, 6].

The Bristol Channel and Severn Estuary is located in the southwest of the UK, with the basin having the second highest tidal range in the world due to the funnelling effect of the basin and tidal resonance [7]. It is therefore not surprising that this basin has been one of the major areas of interest for tidal range schemes [8-11]. Meanwhile, there are areas within the basin which are protected under a number of European and international legislative directives for their unique characteristics and important ecosystem [12]. In recent decades various TRSs have been proposed for siting within the region, but none have yet been developed, due primarily to the potentially significant environmental impacts and the high capital costs [13]. Other concerns reported have related to the need to preserve the delicate inter-tidal mudflats that are vital for migrating birds. Therefore, it is essential to fully understand the performance of such schemes and their environmental and ecological impact on the estuarine waters, both inside and outside of the lagoon or barrage.

The main impacts of TRSs, particularly in terms of the hydrodynamics, are the changes that arise in the water levels and tidal velocities both within and outside of the impoundment, and the consequential impact on the estuarine environment and ecology. For example, changes in the water levels, and particularly the tidal range, as a result of the operation of a TRS can alter the risk of flooding [14] and can cause a significant loss of intertidal mudflats, particularly within the impounded area. Any pronounced loss of intertidal habitats can significantly restrict feeding opportunities for birds post development [15, 16]. Alterations to the tidal hydrodynamics can also significantly impact on solute and suspended sediment concentrations in the estuary, thereby affecting the geomorphological and benthic environments [2, 17-19]. Thus, predicting the impacts of any such scheme on the tidal elevation and velocity characteristics in an estuarine basin are essential in order to assess the preliminary analysis of the design and operation of a new TRS proposal.

Changes in the hydrodynamic regime caused by the operation of a TRS can have both positive and/or negative impacts on solute fluxes and concentrations [20-23]. The impact of such a coastal scheme can significantly affect the water quality characteristics during the initial stages of the design, with such impacts being investigated through predicting the water renewal capacity and water renewal time [24, 25]. However, very little research has been undertaken and reported in terms of the water renewal capacity of TRSs.

There are several ways in which turbines and sluice gates can be represented in numerical hydrodynamic models. In early studies, turbines were modelled in a simplified way by only considering mass-balance through the impoundment wall [10, 26]. However, recent research results have indicated that accurate representation of the lagoon boundary, and particularly achieving accurate momentum conservation of flow through the turbines can have a significant impact on the wake hydrodynamic characteristics, and can be critical in studying the hydro-environmental impact within and in the near-field outside of a lagoon or barrage [27, 28]. Conserving the momentum flux through turbines requires a particular treatment of the momentum terms to ensure conservation, based on the characteristics of the structure [29]. Early studies in treating the momentum flux through the turbines have involved refining the cross-sectional area of the grid cell wall normal to the turbine efflux, thereby ensuring that the velocity exiting from the turbine diffuser cell interface leads to area mean momentum conservation [27]. This paper has adopted a full momentum conservation approach [28] in modelling the flow through the turbines in the lagoon and the impact of different velocity profiles at the turbine outlets have also been studied.

The paper also focuses on studying the hydro-environmental impacts of the proposed West Somerset Lagoon (WSL), with this project being one of the largest lagoon proposals currently being considered in the UK. The scheme design has been optimised for maximum electricity generation with pumping and is expected to generate 7.16 TWh/year [30]. However, this study does not focus on energy generation optimisation and therefore does not include pumping. Another innovation of this paper is the investigation of the operation of WSL on the flushing characteristics within the region by studying the impact on a passive mass-conservative tracer in the lagoon. The corresponding model comparisons for tracer concentrations within and across the lagoon enhance our understanding of the performance of the WSL scheme and encourage maintenance of good water quality characteristics. The impacts of the lagoon on water levels, velocities, intertidal mudflat and bed shear stresses have been studied and are reported herein. The findings from this study have shown that the WSL performed well during this preliminary design study, while showing that further hydro-environmental impact studies and more extensive geomorphological, environmental and ecological modelling studies are also required.

2 West Somerset Lagoon

West Somerset Lagoon was proposed by Tidal Engineering and Environmental Services Ltd (TEES) [31]. The proposal includes a semi-circular breakwater with a length of 22 km, as shown in Fig. 1 and Fig. 2. WSL spans from Culvercliff in Minehead, on the Western end, to West Quantoxhead, on the Eastern end, and encloses an area of approximately 80 km^2. The location of the turbine housings and sluice gates were distributed uniformly initially, while subsequently they have been adjusted to account for local bathymetric and geological conditions, with further studies being undertaken to investigate the optimal environmental considerations and impacts. Based on optimization studies carried out previously at Cardiff University, using a flexible operation of the turbines and based on the findings obtained from a Genetic Algorithm model, the initial layout for the WSL incorporates 125 bulb turbine generators, each of 7.2 m diameter, split equally between 5 housing blocks [30]. The capacity of each turbine is 20 MW, with a total installed capacity of 2.5 GW. To enhance the power output and the flushing capacity, 8 sluice gate housing blocks, with 2 different sizes, have been proposed. The sluicing area of each housing block is: 2860 m^2 for S1-S5 and 1900 m^2 for S6-S8. In total, the proposed sluicing area for WSL would be 20,000 m^2. The locations of the hydraulic structures are shown in Fig. 2, with T1 to T5 illustrating the location of the 5 turbine housing blocks and S1 to S8 representing the 8 sluice gate blocks.

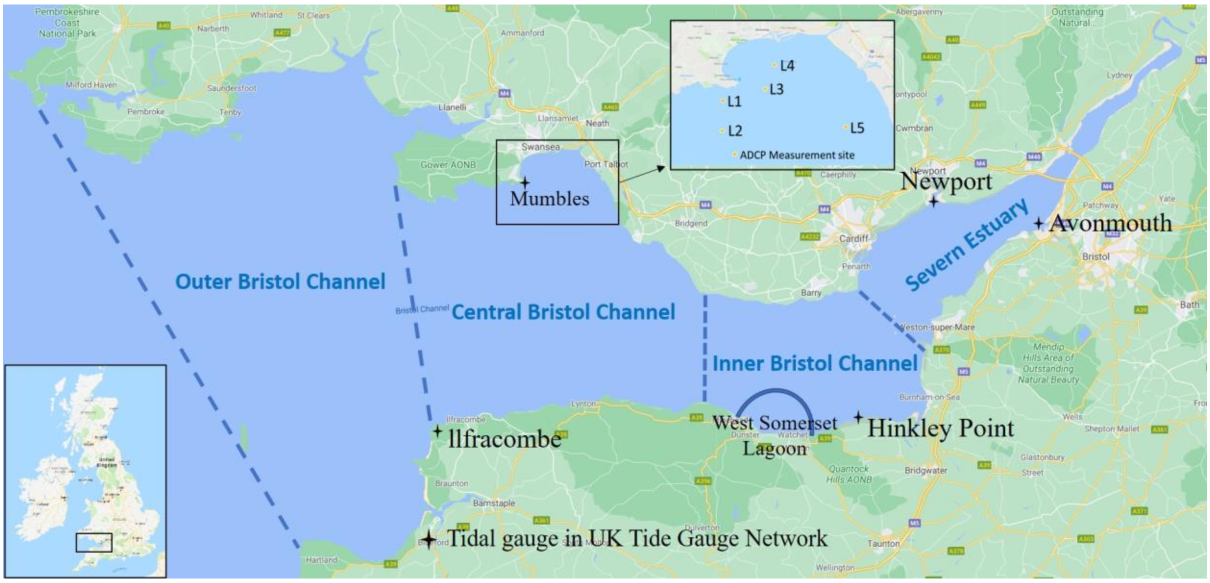

Fig. 1. Location of WSL and model validation data measurement points, including tidal gauge sites and ADCP measuring points.

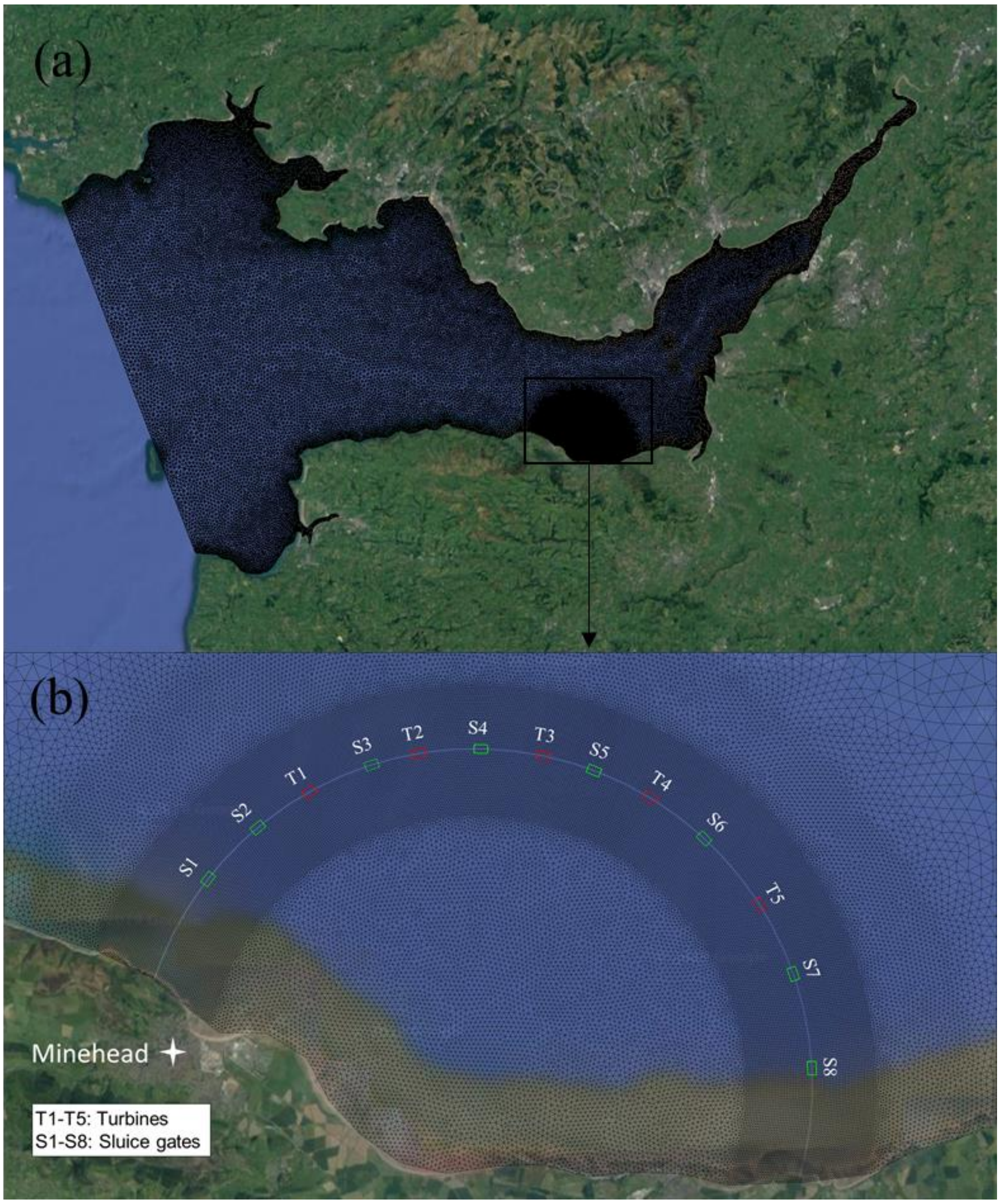

Fig. 2. (a) The computational domain of the model; (b) layout of the turbine housing and sluice gate blocks around West Somerset Lagoon, together with the numerical model grid structure.

TRSs have different operation modes and operating parameters including pumping, which should aim to maximise the energy and minimise the environmental and ecological impact. In order to reduce the loss of basin inter-tidal habitat and to increase net energy output, the WSL scheme (as proposed by TEES) includes pumping but this has not been included in this research. In this study, two different two-way generation scenarios without pumping, and derived from a Genetic Algorithm model, were used as the operation methods for WSL [30]. The first operation scheme was based on the traditional two-way operation of the turbines, with an optimised fixed generation head, and with the energy generation start and end heads being 4.9 m and 2.5 m respectively. The second scheme considered was based on two-way operation with an optimised flexible generating head [32]. The main difference between these two schemes is that the flexible generation head scheme takes account of the fluctuating maximum and minimum sea level for the tidal cycle into consideration, achieving the maximum total energy output by using an adaptive flexible generating head. While a fixed generation head uses a constant turbine start and end parameter throughout the whole tide cycle, this scheme does not take account of the difference between the tidal range for neap and spring tides. It should be noted that optimisation for a flexible head is sensitive to the tidal levels and therefore in the current study the tidal levels in the Bristol Channel were predicted using the model set-up for this study, i.e. TELEMAC, rather than the DIVAST model [32], which was used in the optimised scheme studies.

In considering two-way fixed generation as an example, when the water level inside the lagoon reached its highest level, both the turbines and sluice gates were closed to hold the water volume inside the lagoon. This is termed the holding phase at high tide. The water head difference across the lagoon wall then increases with the receding ebb tide as the tidal level outside of the lagoon falls. When the water head difference is greater than the generation head, i.e. 4.9 m in this case, then the turbines start operating and the ebb generation mode commences. During ebb generation, the water level inside the lagoon keeps dropping until the water head is smaller than the end generation head, i.e. 2.5 m. When this end generation head is reached then the lagoon begins emptying further and the sluice gates are fully open; this is termed the sluicing phase. During this phase, the turbines stop generating and remain idle. This process allows the lagoon to empty as much as possible at low water, thereby creating the maximum head difference for the next generation phase and replicate the natural tide as much as possible to minimise the environmental impacts of the scheme. When the water level is almost the same on both sides of the lagoon wall, the turbines and sluice gates are closed and the holding phase commences again at low water. The water level inside the lagoon stays almost constant again while the water head outside begins increasing. Flood generation starts again when a head difference of 4.9 m is achieved and the ebb tide cycle is repeated. The flexible generation process is similar to the fixed head process, but has the benefit of optimising the energy generated for each individual tide, with the tidal range in any estuarine basin varying continuously. The key operational modes of: holding, generating (or turbining), sluicing and pumping will have different optimal starting and ending heads depending on the tidal range for an individual tide, and the tidal range of the proceeding and subsequent tides. Therefore, to acquire the maximum energy over a spring-neap cycle for any tidal range scheme it is desirable to vary, through optimisation, the starting and minimum heads for each individual tide within the cycle. Further information about the operation of TRSs can be found in Baker [33] and Xue et al. [32].

3 Methods

3.1 Numerical model

In this study, the numerical modelling of the hydrodynamics and the operation of the tidal lagoon has been undertaken using the widely used TELEMAC model. This model is an open-source hydroinformatics modelling suite, developed by the Research and Development Department of Electricite de France (EDF). The TELEMAC suite has been developed to model the hydrodynamics, including the free surface variations and the tidal currents, as well as the hydro-environmental impacts, with the modules including both 2D and 3D hydrodynamic and environmental coupling. The current patterns in the vicinity of the turbines and sluice gates are fundamentally three dimensional in structure [34] and the impact of tidal energy extraction on the water renewal capacity is also a 3D phenomenon [35, 36]. However, 3D modelling of the scheme at this stage would have required excessive computational resources and would potentially have necessitated limiting the simulation period and reducing the horizontal grid resolution. Furthermore, the flow structure in the Bristol Channel is well mixed [37, 38] and the main focus of this study is preliminary on the far-field environmental assessment of this proposed scheme. It was therefore decided to refine TELEMAC-2D in this study due to the well-mixed nature of the estuary [37, 38], computational efficiency and general applicability of the results [28, 39]. However, a 3D analysis of the water renewal capacity will be undertaken in future planned studies.

The Reynolds Averaged Navier Stokes (RANS) equations were solved in the TELEMAC-2D model and the governing depth-averaged equations, written in their non-conservative form [40], are given as:

$$\frac{\partial h}{\partial t} + \vec{u} \cdot \overrightarrow{grad}(h) + h\, div(\vec{u}) = S \qquad [1]$$

$$\frac{\partial u}{\partial t} + \mathrm{u}\frac{\partial u}{\partial x} + \mathrm{v}\frac{\partial u}{\partial y} = -g\frac{\partial Z}{\partial x} + \frac{1}{h}\, div\left(h v_e \overrightarrow{grad}(u)\right) + F_x \qquad [2]$$

$$\frac{\partial v}{\partial t} + \mathrm{u}\frac{\partial v}{\partial x} + \mathrm{v}\frac{\partial v}{\partial y} = -g\frac{\partial Z}{\partial y} + \frac{1}{h}\, div\left(h v_e \overrightarrow{grad}(v)\right) + F_y \qquad [3]$$

where h is the total depth of flow (m); Z is the of free surface water elevation, positive above datum (m); u, v are the depth-averaged velocity components in the x, y-directions (m/s); v_e is the depth-averaged eddy viscosity (m^2/s); S is the mass source term (m/s); F_x, F_y are the momentum source terms representing the effects of wind, Coriolis acceleration, bottom friction, and sources or sinks of momentum.

3.2 West Somerset Lagoon modelling

First, a base-line model was built to simulate the hydrodynamics in the Bristol Channel and Severn Estuary. The open seaward boundary was set at the mouth of the Bristol Channel, spanning from Heartland Point in south-west of England to Stackpole Head in south west Wales, as shown in Fig. 1 and with the seaward boundary conditions being derived from the continental shelf model [41]. It was considered that there was sufficient distance between the seaward boundary and the scheme to ensure limited impact from the scheme on the open seaward boundary conditions for such an early stage study [42]. However, further studies to confirm that the scheme does not have a significant impact on the open seaward boundary will be undertaken at a later date. The model extended upstream to the River Severn, close to the tidal limit at Haw Bridge, near Gloucester, and where there is an Environment

Agency hydrological monitoring station. Major rivers discharges within the domain were included in the model as external sources, with the values for the discharges being based on a report by Stapleton [43]. The entire computational domain covered an area of 5805 km^2. A typical spring-neap tidal cycle, covering the period from 14:00 on 12th August 2012 to 14:00 on 27th August, was used as the baseline for optimizing the scheme, plus two more days at the beginning of the simulations to achieve model set-up conditions. The mesh resolution varied across the domain according to the bathymetric conditions, with the inverse distance interpolation method being used to achieve a higher resolution and better accuracy in shallow waters, with the resolution being based on the following equation:

$$\text{Mesh Resolution} = -10 \cdot \text{Bathymetry} + 200 \quad [4]$$

This method has been used successfully in previous studies for macro-tidal modelling [44] and island wake modelling [45]. Moreover, the mesh was further refined in the proximity of the WSL location, where a finer resolution of the hydrodynamic predictions was required. In summary, the mesh resolution varied from 50 m near the lagoon structure to 800 m close to the open seaward boundary. The computational domain contained 69404 nodes and 134674 elements.

In this numerical model, the method of characteristics was used to solve the advection terms in the governing momentum equations. Discretization in space was carried out by using a quasi-bubble triangle to determine the velocity field and a linear triangle to determine the water elevations, thereby ensuring a balance between model accuracy and efficiency. For turbulence modelling, the classic k-ε turbulence model was used, as this model has been found to be most suitable for modelling flow around obstructions in a macro-tidal estuary and with a conjugate residual solver being adopted [45].

WSL was represented in the model as an independent subdomain, using domain decomposition [10, 39, 46], and in accordance with the actual scale. This meant that the lagoon wall acted as a solid impermeable boundary, except for the turbine and sluice gate sites. The turbines and sluice gates, connecting the internal and external domains either side of the lagoon wall, were represented in the model as an internal discharge boundary, represented by the source term S in equation [1]. The value of the discharge at each timestep was determined as a function of the water head difference across the impoundment wall. This value was added to the domain on one side of the wall and then subtracted from the domain on the other side, thereby ensuring mass conservation. For a submerged sluice gate, a standard orifice equation was used to calculate the discharge as given by:

$$Q_{sluice} = C_d A_{sluice} \sqrt{2g\Delta H} \quad [5]$$

where ΔH is the water level difference across the lagoon wall; A_{sluice} is the sluicing area; and g is the gravitational acceleration. At the preliminary stage of the design and in the absence of any experimental data, the discharge coefficient, C_d, was assumed to be 1.0 [33].

The performance of the turbines, including the flow-through discharge and the power generated, was obtained using a publicly available hill-chart [5, 33, 47, 48]. A hill-chart is unique for different types of turbines and is usually provided by the manufacturer. Due to commercial confidentiality, it has not been possible to acquire the latest hill-chart for the most recently promoted triple regulated turbines. In the current study a typical hill-chart, corresponding to the Andritz Hydro double-regulated bulb turbine, was therefore used [49]. To represent the gradual operation of the sluice gates and turbines, a ramp function was applied to the area, e.g. A_{sluice} in Equation 5. The ramp function represents the physical opening of a sluice gate or turbine and has been expressed in the model in a half sinusoidal form. Thus for the opening operation the function was given in the following form: $f = \sin(\pi t/2T)$, $0 < t \leq T$, and likewise a half cosine form was used for the closing operation: $f = \cos(\pi t/2T)$, $0 < t \leq T$ [50], where T is the time of opening and closing and was assumed to be 20 mins in the current study.

The tidal conditions, i.e. time and height of the tides, are different at each of the turbine and sluice gate blocks shown in Fig. 2, as the tide propagates into and out of the Bristol Channel and past WSL. This variation in the tidal conditions is due to the size of the lagoon and the highly variable tidal conditions in the region, resulting in a 10-20 min difference in the time of the HW (High Water) along the lagoon wall and a difference of 0.2-0.3 m in the spring tidal range between T1 and T5. This variation was expected to affect the optimisation and operation of the scheme and it was found that all the turbines and sluice gates, following the same opening and closing rules, as determined by a single water level inside and outside of the basin - as traditionally used, led to an inefficient performance of the scheme [19, 28]. Therefore, the optimisation of the scheme was carried out by separately operating each component, i.e. turbine and/or sluice gate block, using water levels predicted by TELEMAC-2D at the location of each block structure. The model was then revised to operate each structure independently, which led to an improved and more efficient operation of the scheme for the 2D and 0D model, as discussed further in section 4.2.

3.3 Momentum conservation across the structure

To ensure momentum and mass conservation across the structure, a momentum source term was added to the momentum equations, i.e. Eqs. 2 and 3, for the cells linked to the turbines or sluice gates. This method has been successfully used in simulating tidal stream turbines [51] and is applicable to other hydraulic structures, such as coastal reservoirs [52]. The momentum source term in the x direction was calculated from first principles and is given as:

$$F_x^q = \frac{1}{h}(u_s - u) \cdot S = \frac{1}{h}(u_s - u)\frac{Q}{(\Delta\xi \times \Delta\eta)} \quad [6]$$

where $\Delta\xi \times \Delta\eta$ is the area of the source/sink discharge; u is the local velocity at the source point, h is the water depth; and u_s is the jet velocity through the source point, which was considered as the flow velocity through the hydraulic structure, as shown in Figure 3. However, due to the fast-changing velocity in the turbine housing [53], the value selected to define u_s is uncertain. Therefore, different values of u_s were applied and compared in this study. In the first scenario, the velocity was taken just beyond the turbine runner, which could be considered as a simplified value since this value ignored the expansion of the flow through the diffusor [28]. In the second scenario, the value of u_s was considered as the velocity at the end of the turbine diffusor. This was considered to be more realistic, based on Eq. 6, and includes the energy dissipation in the draft tube.

Vertical velocity gradients cannot be accurately accounted for in 2D models [26] for such complex turbine wake structures and u in Equation 6 was derived from the model. However, the velocity of the jet, u_s, can vary significantly over the diffuser. This hydrodynamic jet will be different based on the design of the turbine and its housing and therefore an appropriate velocity profile needs to be used after the turbine characteristics have been finalized. However, at this early stage of the design process, a typical horizontal velocity profile along the vertical section produced by Wilhelm et al. [54], as shown in Fig. 3, was used in this study. The velocity profile is represented in Eq. 6 by dividing the profile into small sections and calculating the accumulated impact of the jet over the area, as shown below:

$$F^{q}_{x-3D} = \frac{1}{h(\Delta\xi \times \Delta\eta)} \int_0^h (u_s - u) Q dZ \qquad [7]$$

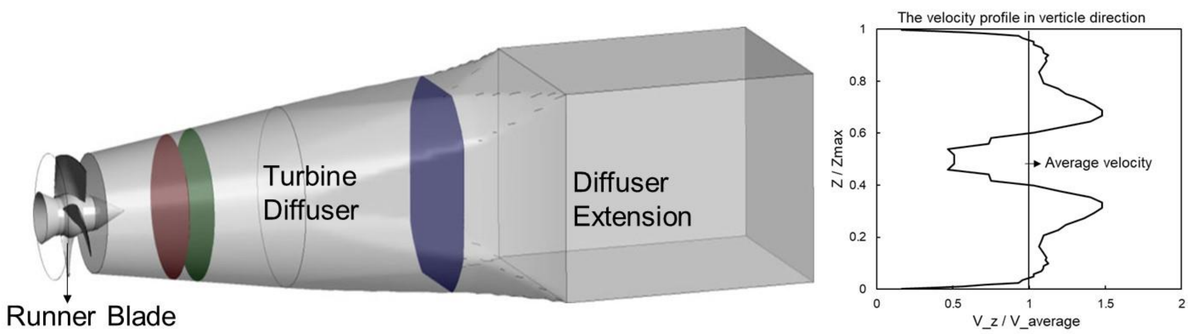

Fig. 3. Shape of the low head bulb turbine housing and measured velocity distribution in the outer turbine diffuser [54]

3.4 Renewal time and bed shear stress calculation

In order to study the water retention time of WSL, the renewal time was estimated by studying the characteristics of a passive mass-conservative tracer, which was introduced inside the lagoon domain. This tracer was then monitored to give the concentration changes with time, particularly inside the lagoon. It is also known that the renewal time depends on the tracer release time during a tidal cycle and different calculation methods of renewal time were applied [24, 25, 55, 56]. For the current study, the tracer was introduced at low-water for a typical spring tide, with the tracer being released instantaneously within WSL and dispersed uniformly. A tracer remnant function was adopted to represent the remaining tracer in the studied domain [57], as follows:

$$r(t) = \frac{\int_\Omega h(x,y,t) \cdot T(x,y,t) d\Omega}{\int_\Omega h(x,y,t_0) \cdot T(x,y,t_0) d\Omega} \qquad [8]$$

Where x, y are the spatial coordinates; t_0 is the initial time of tracer releasing; h is the water depth and T is the tracer concentration. The renewal time was then determined based on the method proposed by Matta et al.[24] and Guillou et al.[55], in that the renewal time was taken as the time when the average tracer concentration across the lagoon dropped by 10% of the initial concentration.

The impact of the lagoon on sediment transport, including potential erosion and deposition changes, and particularly long-term geomorphological changes, was another key concern for such a scheme. The bed shear stress is a major indicator of potential changes in sediment transport and hence the bed shear stress was predicted and compared in the region for pre- and post- lagoon construction of the lagoon. The bed shear stress was calculated using a conventional quadratic formulation, as given by:

$$\tau = \rho C_d |u| u \qquad [9]$$

where ρ is the seawater density, assumed to be 1025 kg/m^3, C_d is the bottom drag coefficient, assumed to be 0.0025 in this study [58], and u is the depth average velocity and $|u|$ is the magnitude of the depth average velocity.

3.5 Statistical Analysis tool

The coefficient of determination (R^2) and the root mean squared error (RMSE) were used to quantify the predictive capability of the model when validated against measured water level data, with the terms being defined as:

$$R^2 = 1 - \frac{\sum_{i=1}^{n}(S_i - O_i)^2}{\sum_{i=1}^{n}(O_i - \bar{O})^2} \qquad [10]$$

$$RMSE = \sqrt{\frac{1}{n}\sum_{i=1}^{n}(S_i - O_i)^2} \qquad [11]$$

where O_i is the observed value, $\overline{O_i}$ is the average of the observed value, S_i is the simulated value, and $\overline{S_i}$ is the mean of the simulated value. The R^2 and RMSE values are mainly applied to evaluate scalar quantities, not vector quantities. Thus, the mean absolute error (MAE) and relative mean absolute error (RMAE) were also evaluated for quantifying the degree of accuracy of the model in predicting the measured velocities. The MAE contained both errors of magnitude and direction, with the formulation for a vector $\vec{X} = (X_1, X_2)$, being given for MAE and RMAE as follows:

$$MAE = \langle |\vec{S} - \vec{O}| \rangle = \frac{\sum_{i=1}^{n}\sqrt{(S_{1n} - O_{1n})^2 + (S_{2n} - O_{2n})^2}}{n} \qquad [12]$$

$$RMAE = \frac{MAE}{\langle |O| \rangle} \qquad [13]$$

The qualification for the ranges of RMAE is also presented , with: Excellent (RMAE < 0.2), Good (0.2 ≤RMAE < 0.4), Reaonable (0.4 ≤ RMAE < 0.7), Poor (0.7 ≤ RMAE < 1.0), Bad (RMAE ≥ 1.0) [59].

4. Result

4.1 model calibration and validation

The model was first calibrated using water level and velocity data from the Admiralty Charts [10] and 4 tidal gauges covering the Bristol Channel and Severn Estuary. A manning's roughness coefficient of 0.025 was selected during calibration, which was generally found to give the closest agreement between the predicted results and available field data. The model was then validated using further tide level gauges and ADCP measured data.

Sea surface elevation data obtained from four British Oceanographic Data Centre (BODC) tide level gauges, including: Avonmouth, Hinkley Point, Mumbles and Newport (shown in Fig. 1), were used for model validation. The comparisons between the model predicted water levels and the measured data are summarized in Table 1; comparisons of the water levels at the nearest gauge to the WSL site, i.e. Hinkley Point, are shown in Fig. 4. The comparisons between the predicted and measured water levels and velocities show good agreement. All of the R^2 results show a strong correlation between the model predicted and measured free surface elevations, thereby giving confidence in the accuracy achieved using the model for predictions for the preliminary design. Although the water levels at Newport show a slight misalignment, this is thought to be due to the relatively shallow water depths and the complex bathymetry in the vicinity of the tidal gauge. Available seabed mounted ADCP monitoring sites are also shown in Fig. 1, with these sites providing velocity data for further model validation. A typical comparison of water level and current speed/direction values at point L3 are shown in Fig. 4, with a statistical analysis of these comparisons being summarized in Table 1. The R^2 values for the comparisons with the ADCP measured water levels were all higher than 0.99 and the MAEs for both current magnitudes and directions were smaller than 0.1, except at site L1. Three of the RMAE indicator values were classified as being 'excellent' and with the others classified as 'good', according to the classifications given for the RMAE. The validation between the model predicted and the ADCP measurement data therefore show good correlations, again giving confidence in the accuracy of the model predictions.

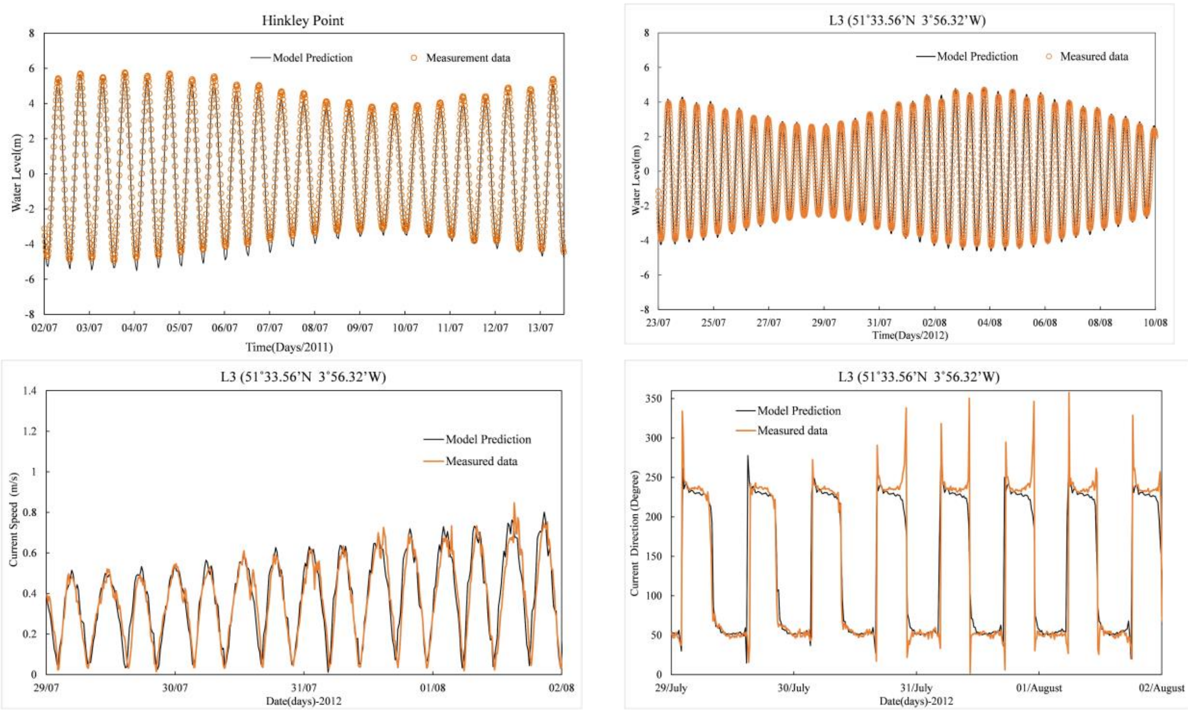

Fig. 4. Typical comparison of water levels, current speeds and directions at one tidal gauge and one ADCP measurement site.

Table 1 Validation statistics of BODC gauge data and Swansea Bay ADCP data

Water level analysis		
Site	RMSE (m)	R2
Avonmouth	0.359	0.992
Hinkley	0.351	0.988
Mumbles	0.420	0.964
Newport	0.767	0.932
ADCPs L1	0.260	0.990
ADCPs L2	0.213	0.993
ADCPs L3	0.232	0.992
ADCPs L4	0.231	0.992
ADCPs L5	0.214	0.993

Swansea bay ADCPs measured Velocity magnitude		
Site	MAE (m/s)	RMAE
ADCPs L1	0.122	0.222
ADCPs L2	0.083	0.145
ADCPs L3	0.057	0.142
ADCPs L4	0.045	0.191
ADCPs L5	0.076	0.230

The tidal constituents were then used to validate the model and to explore the tidal resonance characteristics in this area. The model was run for more than 30 days, to achieve an accurate harmonic analysis. The Matlab package T-tide [60] was utilized to derive the tidal constituents. The top three dominating tidal constituents were M2, S2 and N2 and these were compared using the BODC tidal measurements and model predictions, with the resulting comparisons being summarised in Table 2.

The corresponding results show that the amplitudes and phases for the M2, S2 and N2 tidal constituents are all well matched and most of the agreement between both sets of results is less than 5%. However, the M2 phase shows a discrepancy at the Ilfracombe site, where the discrepancy is more than 8%. The Ilfracombe gauge is sited closest to the seaward boundary, which suggests that there might be some small impact from the seaward boundary conditions. In comparing with the harmonic analysis results in this area with the findings of other researchers the results show that the harmonic components data are close to the published findings, further confirming that the validation agreement is encouraging [61, 62].

Table 2 Amplitude and phase comparisons for M2, S2 and N2 tidal constituents at 5 gauges

Tidal gauges		M2 Amplitude(m)	M2 Phase (deg)	S2 Amplitude(m)	S2 Phase (deg)	N2 Amplitude(m)	N2 Phase (deg)
Hinkley	Observation	3.80	185.0	1.42	237.0	0.62	171.75
	Prediction	3.78	187.2	1.52	246.1	0.59	176.1
	Difference	0.5%	1.2%	7.0%	3.8%	4.8%	2.5%
Mumbles	Difference	0.56%	-4.15%	-2.82%	-1.04%	12.26%	-3.93%
Ilfracombe	Difference	0.15%	-8.84%	-4.11%	-3.82%	-3.10%	-1.70%
Newport	Difference	1.96%	-9.35%	-1.63%	-4.79%	1.57%	-2.75%
Avonmouth	Difference	-0.38%	-5.96%	-5.45%	-3.50%	-4.83%	-1.70%

4.2 Lagoon operation for two-way generation

The model predicted water levels inside and outside of the lagoon, the flow through the turbines and the power generated are all shown in Fig. 5. The total energy generated during a typical spring-neap cycle for fixed and flexible generation schemes were predicted to be 0.196 TWh and 0.233 TWh, respectively. The energy generated over the typical cycle can then be multiplied by 24.6 to provide the annual generation [30]. This gives 4.82 TWh and 5.73 TWh per annum for fixed-head and flexible head generation, respectively. The advantage of the flexible head generation scheme, which can yield up to 19% more energy, with no additional investment, is noticeable from these results. These results are also consistent with similar 0D model predictions, used to optimise the scheme, and giving comparable predictions of the annual energy output of 4.87 TWh and 5.71 TWh for fixed-head and flexible head generation, respectively and leading to differences of 1% and 0.35% for annual energy outputs for fixed-head and flexible head generation, respectively. This confirms that the simplified 0D model simulated the operation well for the WSL and hence this operation scheme could be used for the 2D modelling [30].

The significant increase in energy generated for optimised flexible head generation compared with traditional fixed head generation showed the benefit of adopting a flexible head generation operational procedure for the turbines and sluice gates. By comparing the discharge and power outputs in Fig. 5, it is noted that the optimised generation scheme delayed the turbine generating time to achieve a higher turbine working head. Although a small increase in the water level difference and the discharge is predicted, the extra energy generated is significant due to the approximate square relationship between power and water head difference in tidal range energy extraction [30].

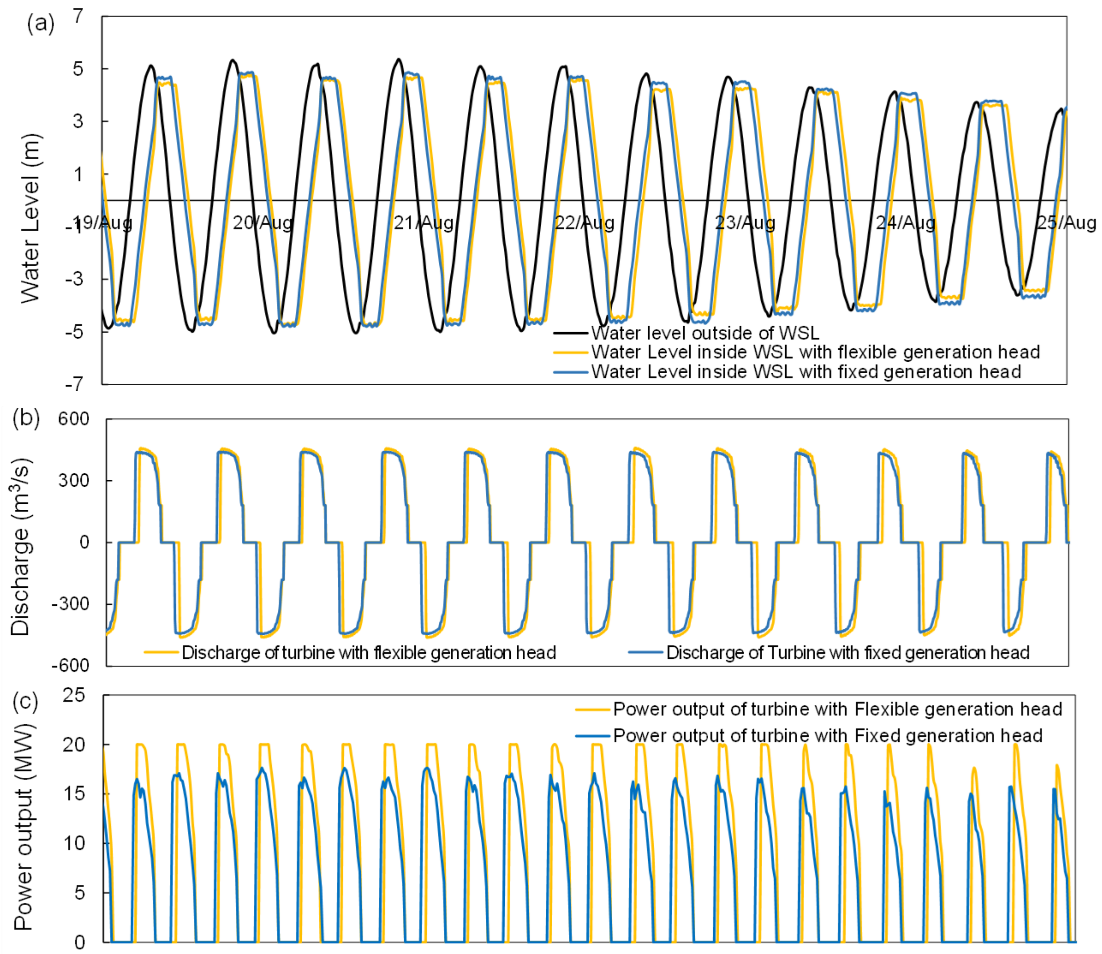

Fig. 5. (a) Water level variations for lagoon operation; (b) discharge through a single turbine; and (c) power output for a single turbine.

Almost all previous hydro-environmental modelling studies undertaken in the past have used a fixed head operation procedure. However, since the flexible generation scheme shows an appreciable increase in the energy generated, when compared to that generated using a fixed generation head procedure, it is likely that the flexible generation scheme will be adopted in further TRSs proposed in the future. The following analysis will therefore be based for two-way generation with the optimised flexible head.

4.3 Different momentum conservation and velocity distribution comparisons

The velocity distributions in the vicinity of the lagoon, for a peak discharge through the turbines and during high spring tide, are shown in Fig. **6**. The comparisons show the predicted variations for three different representations of momentum conservation across the lagoon wall, in the form of an additional source term, and as outlined in section 3.3.

Fig. **6** (a, b) shows the model predictions without any momentum source term included and was taken as the baseline model for comparison purposes. For all cases in Fig. 6 the velocity distribution on the left shows that predicted during a flood tide, with ebb tide predictions being shown on the right. It can be seen that the turbine jet has a length of around 2.2-3.3 km and a core velocity of 1.7-2.9 m/s during flood generation. When the velocity at the end of the turbine diffusor was used to include the momentum source term, it was observed that the turbine jet was slightly increased in comparison with the baseline predicted characteristics, with a length of about 2.5-3.4 km and a core velocity of 2.2-3.2 m/s, as shown in Fig. 6(c). The small difference in the velocity magnitude between Fig. 6(a) and (b) and Fig. 6(c) and (d) means that the original velocity at the outlet of the turbine diffuser was predicted to be slightly smaller than the source velocity taken at the turbine diffuser. A higher turbine jet velocity is predicted in Fig. 6(e), reaching up to 3.3 m/s and with the length of the turbine jet reaching 2.7-3.7 km.

The turbine jets for ebb generation show similar overall results to those predicted for flood generation. Moreover, it is noticeable that the water jet through the turbine block T5, the most easterly block, is clearly more pronounced than the jets effluxing from the other blocks. This is mainly caused by the relatively shallower bathymetry to the east of WSL, and the resulting slightly larger water head difference of 0.2-0.3 m through this block complex shape, and the strong degree of resonance in the Bristol Channel and Severn Estuary.

The eddy structure also changes with the different momentum source term representations. For example, circulation zones appeared on both sides of each jet in Fig. 6(e), which arose as a result of the higher velocity differences. Weaker circulation cells developed in Fig. 6(a) and (c), due to the weaker jet velocities. The relatively high tangential velocities in the inner Bristol Channel, meant that outside of WSL the ebb tide jets were strongly deflected by the tidal currents and eddies were mainly generated only on the western side of the lagoon. This ebb flow structure in the main channel could affect sediment transport processes in the region, although this was not studied in the current investigations.

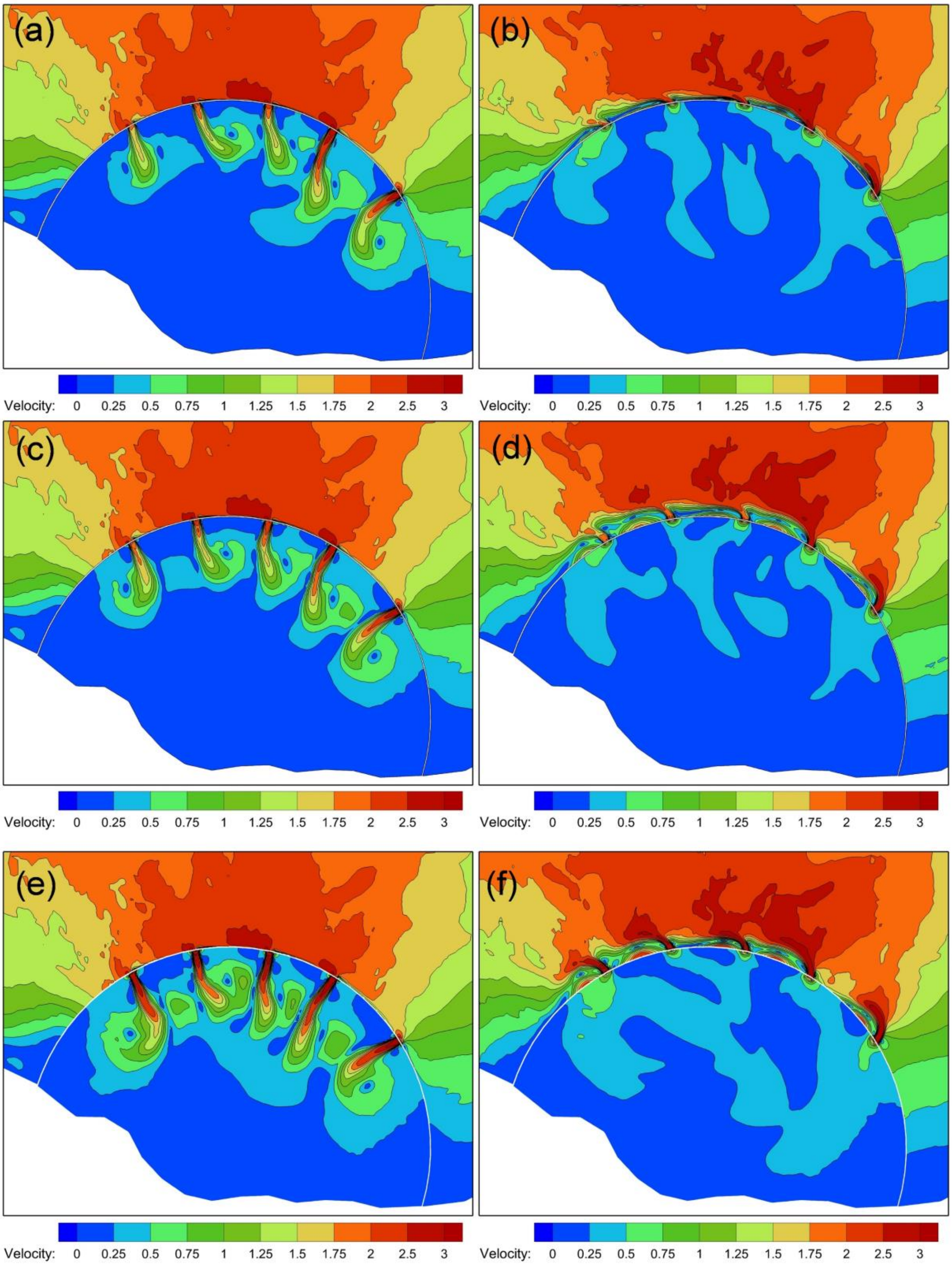

Fig. 6. Instantaneous velocity fields for peak discharges during flood and ebb generation, for a typical spring tide and with different momentum source terms: (a) and (b) model without momentum source term; (c) and (d) model with momentum source using velocity at the end of the turbine diffusor; and (e) and (f) model with momentum using velocity taken at the turbine blade location.

In comparing with the momentum source velocity taken as the depth-averaged velocity and the model with depth-integrated source velocity, the model shows a limited impact on the turbine jet, as seen in Fig.7. This has some influence on the flow pattern near the turbines, but is negligible in the far-field study.

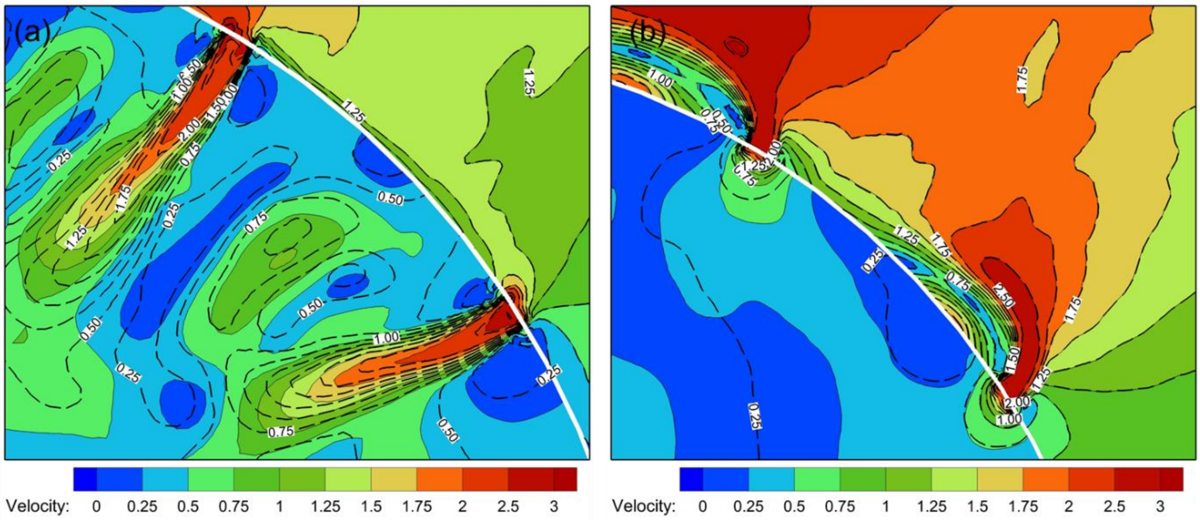

Fig. 7. Turbine jet comparisons between momentum with depth-averaged source velocity (colour contour) and depth-integrated momentum (dotted line) during (a) flood generation; (b) ebb generation.

It is concluded from Figs. 6 and 7 that the introduction of momentum term has a significant influence on the flow pattern near the lagoon. The momentum term with source velocity included at the end of the turbine diffusor was therefore applied in all subsequent lagoon modelling simulations since it was considered to be more representative of the true hydrodynamics in the near-field of the turbines and sluices. However, in modelling the turbine wake and momentum conservation further testing and validation is required in terms of including momentum conservation through comparisons with field observations or experimental studies with a scale physical model of a simplified TRS.

4.4 Hydrodynamic impact analysis

4.4.1 Tide harmonic constituents change

To understand the impact of the lagoon on the water levels, the tidal constituents were studied individually and the results are summarised in Fig. 8. It can be seen that the operation of the lagoon has generally moved the amplitude for the M2, N2 and S2 tidal constituents further into the inner Bristol Channel towards the head of the estuary, and particularly after passing WSL in the upstream direction. Furthermore, for the M2, N2 and S2 phases these were also noticeably affected by the lagoon, again particularly towards the east of the lagoon and up to the Severn Estuary. In other words, WSL has increased the amplitude of these three tidal constituents in the region and particularly to the east of the lagoon and towards the head of the estuary. Likewise, the phase has increased to the West of WSL, while it has decreased to the East. Thus, the influence of WSL on the tidal harmonic constituents is predicted to be greater towards the head of the estuary, which is thought to be particularly pronounced due to the convergence of the estuary and the natural frequency of the Bristol Channel and Severn Estuary.

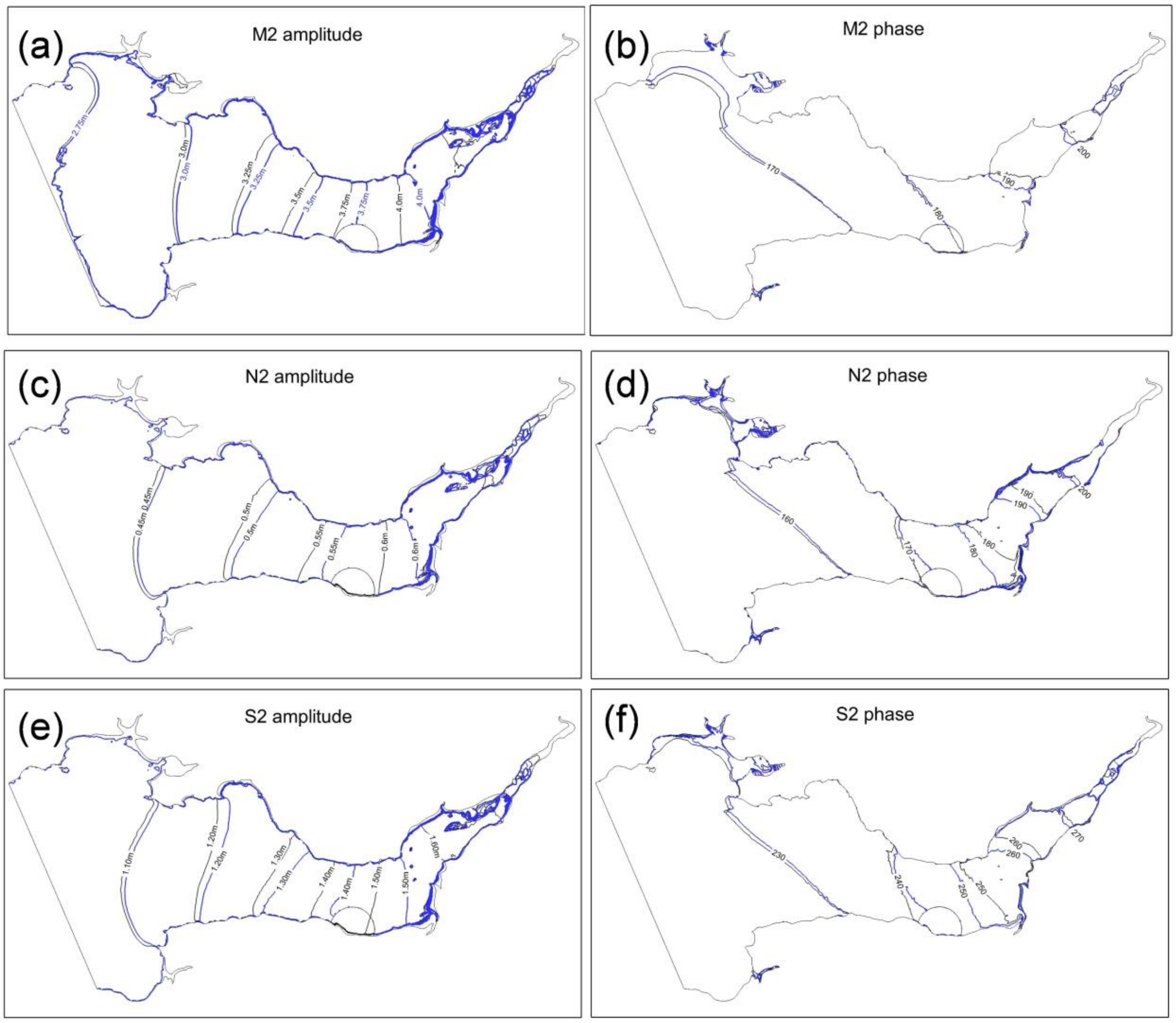

Fig. 8. Comparison of cotidal charts for M2, N2, S2 before and after the construction of WSL. (a),(c) and (e) show the amplitude of M2, N2 and S2; and (b), (d) and (f) show the phase of M2, N2 and S2. (The black line represents the tidal constitutes for pre-lagoon construction and the blue line refers to post-lagoon)

4.4.2 Water level change

The model predictions showed that the highest water levels inside the lagoon dropped by up to 1.2 m as a result of the operation of WSL, as illustrated in Fig. 5(a). Fig. 9 also shows that in the middle and inner Bristol Channel, the water level has dropped by 0.05 - 0.2 m. The changes in the peak water levels across the domain were greater within the Severn Estuary and were predicted to be 0.2 - 0.3 m. The envelope curves of high water levels along the estuary in Fig.10 confirm this phenomenon, in that the high water level upstream of Mumbles decreased for the post-lagoon condition, while the high water level near the open boundary increased slightly. These results suggested that the reduction in flow area across the Bristol Channel at the WSL site had an effect on the resonance characteristics of the tide as it propagated up the Bristol Channel and Severn Estuary.

There are a number of cities and towns and key infrastructures (such as the Port of Bristol) located along the Severn Estuary and Bristol Channel. These predicted changes in the peak water levels are generally small and will only have a modest impact at the various coastal sites and facilities, such as the Port of Bristol. Table 3 lists the high and low water level changes in spring tide (DWHS and DWLS) and neap tide (DWHN and DWLN) at various locations along the basin after the introduction of WSL. For the potential tidal range energy plants, the positive values for DWLS and DWLN and the negative values for DWHS and DWHN means that the tidal range will decrease slightly at several of these sites, which will lead to a small reduction in the estimated energy output at some sites after the construction of WSL.

The critical indicator for shipping is the minimum water level that determines the available time for manoeuvering into docks etc. While a positive value of DWLS for docks refers to an increase in the minimum water level, this means that the shipping industry and leisure yachting etc. could benefit marginally from WSL. Furthermore, the positive DWLN and negative DWHS at the key bird feeding sites would also mean a small increase in the minimum feeding area and a corresponding decrease in the maximum feeding area. Furthermore, the positive DWHS means a drop in the peak water level at some important sites, thereby reducing the relative risk of flooding at these sites.

In considering the predicted changes in the water levels after including WSL, these changes are all relatively small and within the error of measurement at the reported observation gauge sites, as shown in Fig.10. Moreover, for more accurate predictions of the impact of WSL then the open seaward boundary should be extended beyond the existing location and seawards to the Continental Shelf; this would remove any potential impact of the lagoon on the open seaward boundary.

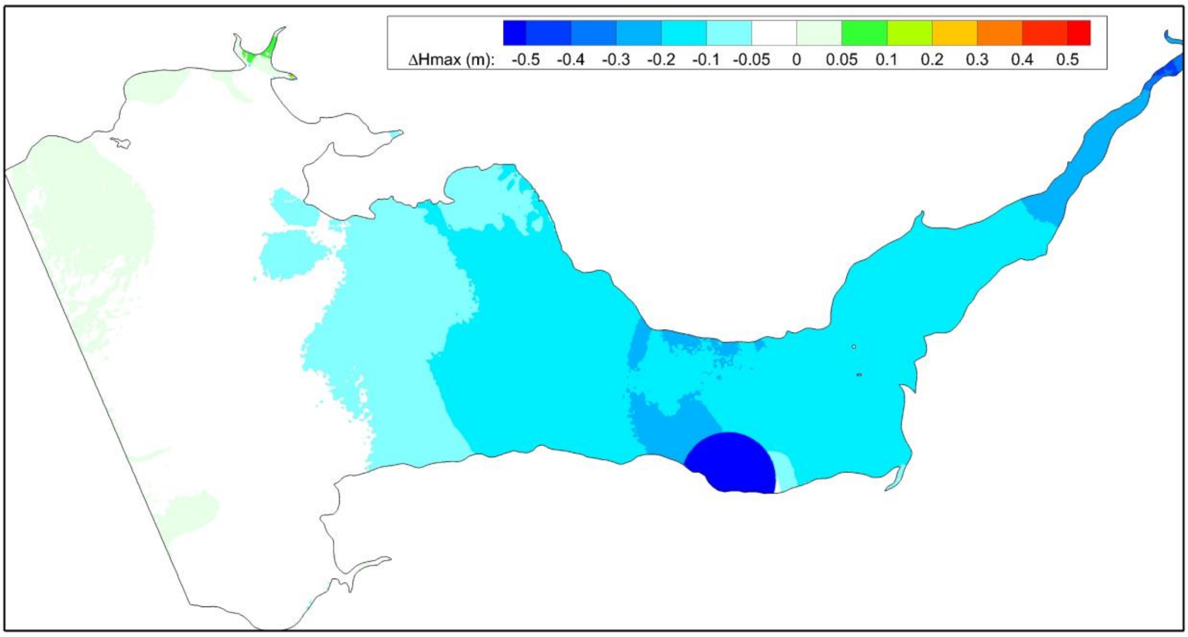

Fig. 9. Cumulative effect of WSL on maximum water level during a spring-neap tidal cycle

Table 3. High and low water level differences with WSL at selected sites in the Bristol Channel and Severn Estuary. (DWHS: Difference in water level at high spring tide; DWLS: Difference in water level at low spring tide; DWHN: Difference in water level at high neap tide; DWLN: Difference in water level at low neap tide)

Site	DWHS(m)	DWLS(m)	DWHN(m)	DWLN(m)
Proposed Lagoon Scheme				
Cardiff Lagoon	-0.165	0.266	-0.070	0.121
Swansea Bay lagoon	-0.094	0.031	-0.019	0.036
Severn barrage	-0.155	0.271	-0.052	0.088
Newport Lagoon	-0.151	0.253	-0.077	0.162
Bridgewater bay Lagoon	-0.141	0.300	-0.054	0.085
The Docks				
Avonmouth dock	-0.156	0.187	-0.086	0.132
Cardiff dock	-0.155	0.198	-0.056	0.072
Swansea dock	-0.091	0.072	-0.008	0.022
Porlock dock	-0.164	0.18	-0.088	0.045
Birds feeding area				
Bridgwater Bay	-0.091	0.256	0.042	0.135
Welsh grounds	-0.154	0.110	-0.103	0.161
Important Sea defences				
Hinkley nuclear power station	-0.094	0.322	-0.015	0.068
Somerest	-0.156	0.040	0.008	0.010
Peterstone flats	-0.157	0.264	-0.071	0.088
Slimbridge	-0.368	0.012	-0.276	0.011

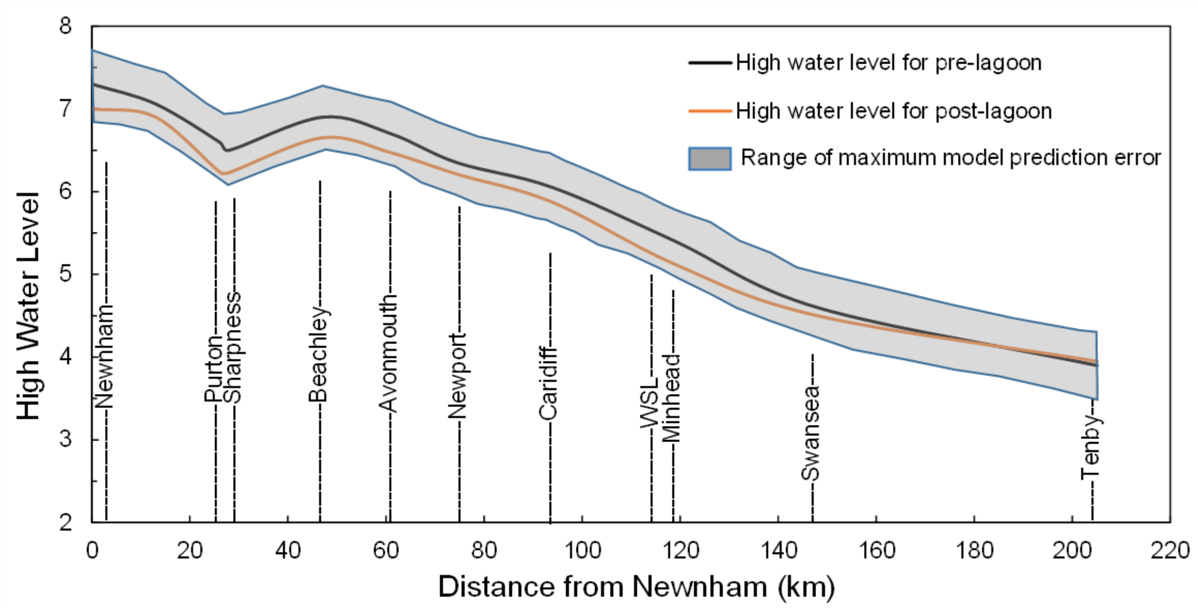

Fig. 10. Envelope curves of high water levels for pre- and post-WSL and maximum predicted model deviation.

4.4.3 Impact on the area of the intertidal mudflats

Changes to the intertidal mudflats zones are considered to be one of the key ecological concerns of tidal range schemes. Intertidal zones are important feeding habitats for birds, mussel and insects, which are crucial for biodiversity in the estuary [63, 64]. Fig. 11(a) shows that the construction and operation of WSL would slightly reduce the maximum intertidal area during low water level for both spring and neap tides, while the minimum area generally would remain unchanged at the same level. The change in area identified in Fig. 11(b) confirmed that WSL could decrease the mudflat area during most of the tide cycle by up to 20 km^2, mainly in the upper Severn Estuary. The loss of the intertidal mudflats is mainly caused by an increase in the predicted low water level, with a slight increase in the water level causing a noticeable decrease in the intertidal area in some parts of the estuary. The changes in the low intertidal areas are shown in Fig.12. It is known that the low intertidal zone is virtually always underwater and only exposed during lowest spring tides, thus the area is abundant with life because of the protection provided by the water [65]. Except for the loss of some of the low intertidal zones within the WSL basin, resulting from the sea level change inside WSL, the low intertidal mudflat region around Welsh grounds, Severn beach and the outer Severn Estuary have all decreased slightly. It should be noted that the changes in these areas are mainly due to the shallow bathymetry and the gentle slope, which makes the mudflats very sensitive to small changes in the lowest water levels. There are some other factors that need to be included for an accurate qualitative prediction of the changes, including: the qualitative change occurring for specific wetland conservation areas, whether the lagoon can be operated specifically to minimise its impact on intertidal mudflats, the period that the intertidal area is submerged within a day and the relationship with bird feeding times. Therefore, further studies are required in the future to identify more accurately the impact of the lagoon, and its operation, on the intertidal mudflats and particularly in the Severn Estuary.

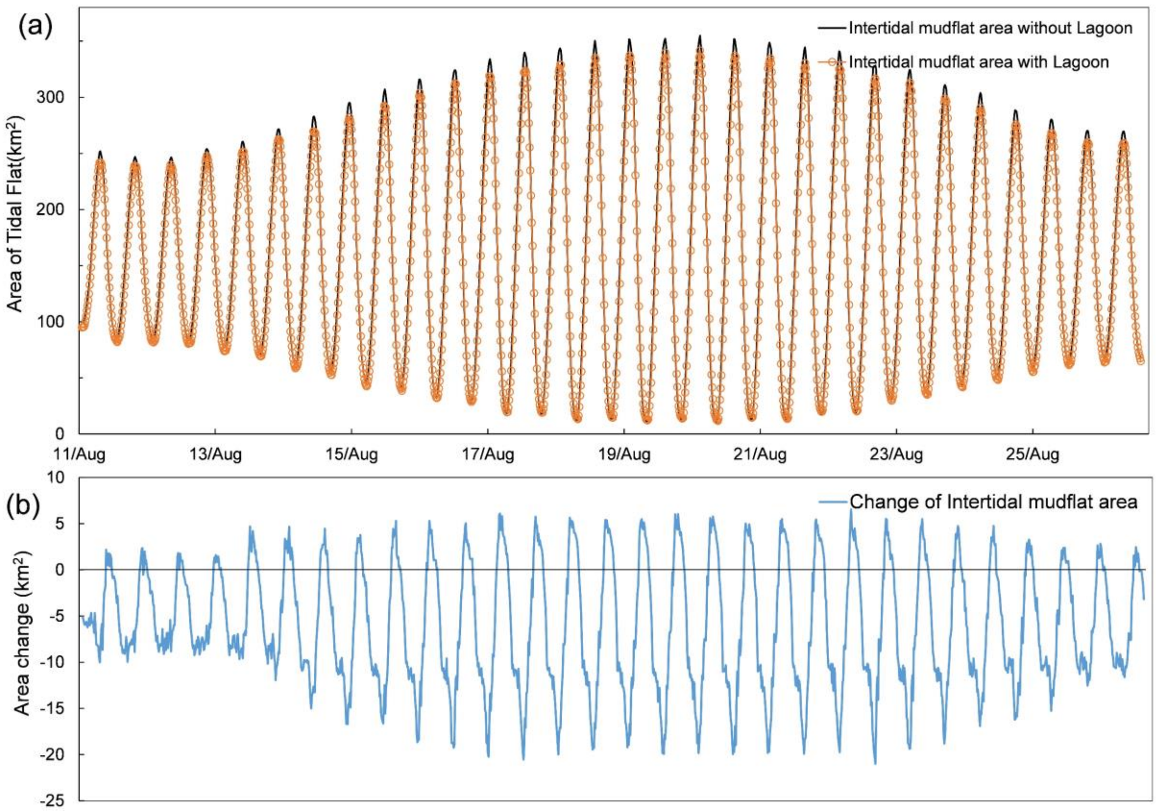

Fig. 11. Change in intertidal mudflat areas before and after the construction of WSL, (a) the area of tidal flat area for pre- and post-WSL; (b) the change in tidal flat area with WSL.

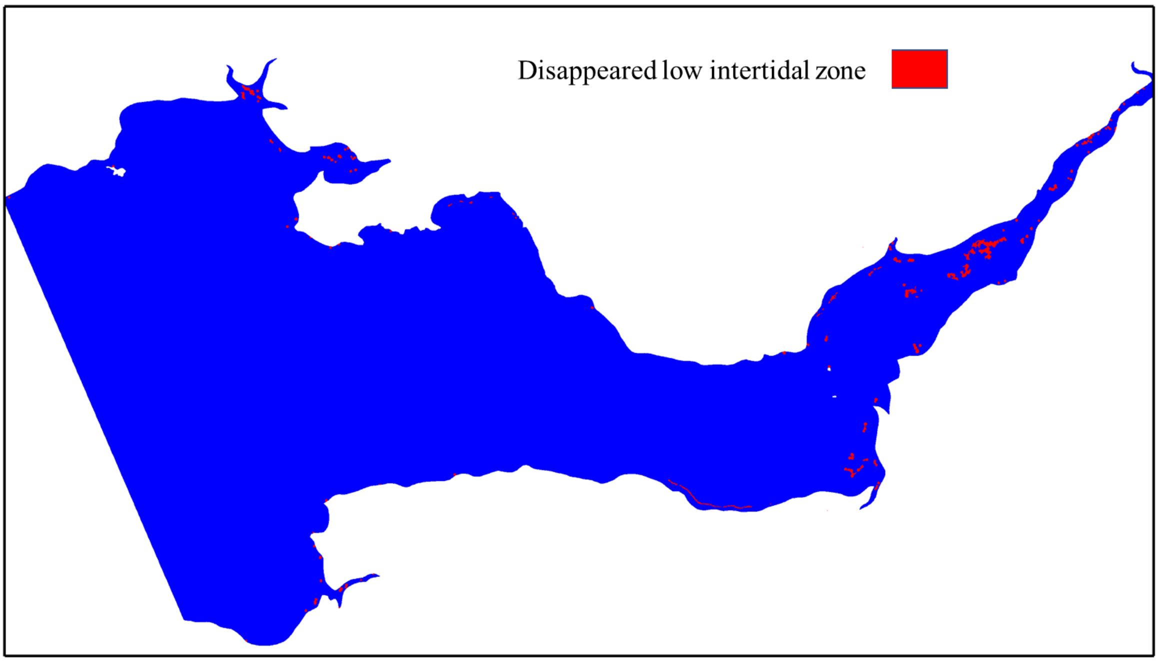

Fig. 12. The loss of low intertidal zone after the operation of WSL.

4.4.4 Changes to velocities

The introduction of WSL structure and the operation of the turbines and sluice gates changes the simultaneous and accumulated tidal currents, to varying degrees, across the model domain. Fig. 13 shows the accumulated impact of WSL on the velocities during a maximum spring tidal cycle. As expected, the existence of a jet at the exit of the turbines and sluice gates results in a significant increase in the accumulated velocity of up to 1.5 m/s, in the vicinity of the turbines and sluices. The corresponding velocities in the inner Bristol Channel, further away from the structure, show a typical increase of 0.25 to 0.75 m/s. These changes in the velocities are more noticeable closer to WSL. This is to be expected due to the blockage effect of the scheme, which reduces the effective cross-sectional area of flow across the Bristol Channel at the lagoon site, thereby resulting in slightly higher velocities in the region. However, the velocities inside the impoundment were markedly reduced except in the vicinity of the turbine and sluice gate wakes. This is consistent with the pattern observed at other TRSs [10, 27, 28, 39] and is primarily due to the limited interaction between the water volume with the basin and the natural flow in the estuary and outside of the lagoon. There is a relatively large area to the West of WSL where the velocity is predicted to be reduced, which contributes to the blockage effect of the lagoon on the freestream flow, as observed around headlands and natural flow obstructions [45, 66]. Moreover, the lower natural velocities on the shallower region to the eastern side of WSL causes a greater increase in the maximum velocity in the vicinity of the turbines and sluice gates in comparison with conditions on the western side of the scheme.

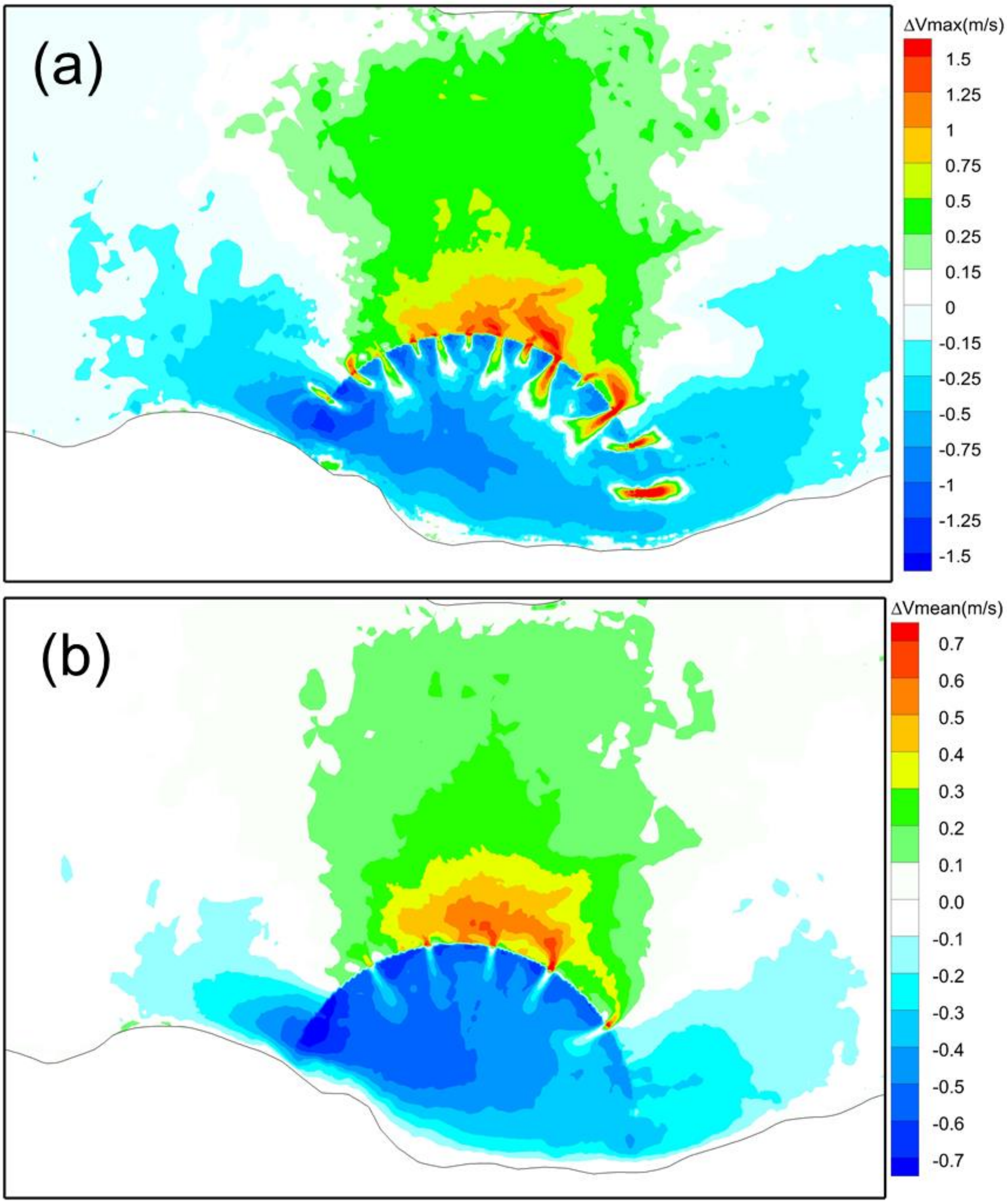

Fig. 13. The cumulative effect of WSL on the maximum and averaged velocities for a spring-neap tidal cycle. (a)ΔVmax is the difference in the maximum velocity and (b) ΔVmean refers to the average velocity difference during the spring-neap tidal cycle.

4.5 Renewal time

The flow pattern within the lagoon and in the region will have an impact on the water retention and renewal capacity, particularly inside the basin, as indicated by the flow patterns in Fig. 13. The behaviour of a passive conservative tracer was used to study these changes [24, 55]. The tracer was first released in the lagoon located at high water level for a typical spring tide. In the first instance the tracer movement was modelled without the lagoon in place, and was flushed freely with the tides and without any restrictions. The tracer concentration distribution after 2 tidal cycles is illustrated in Fig. 14(a). This result shows a significant change in the average tracer concentration in the lagoon impoundment area after release, as seen in Fig.15. This oscillation continues for some time, with the tracer being diluted mostly by the process of dispersion. The renewal time for this natural condition is about 22.4 days. This relatively high renewal time is thought to be due to the magnitude of the ebb and flood tides and the low residual currents in the area [67].

In the subsequent simulations WSL was included in the model, with the flushing processes inside the lagoon being much more confined due to the marked changes in the local velocity patterns arising from the lagoon operation. A comparison of the concentration distributions shown in Fig. 14 (b), (c) and (d) illustrate the impact of the mixing processes on the tracer and the impact of the vortex trapping associated with the jet induced vortices inside the lagoon and induced by the turbine and sluice gate wakes. The larger wakes induce larger and stronger vortices and extend further into the impoundment area, resulting in more mixing. While smaller jets cause less interference with high concentration areas and encourage more of the concentration towards the shoreline. Fig.15 shows that tracer concentrations oscillate to a lesser degree after the inclusion of the lagoon in the model. The momentum conservation through adjusting the momentum source terms tends to have a higher impact on the renewal times. The model renewal time predictions without the momentum source terms, and with realistic source velocity and simplified source velocity momentum adjustments, were 9.75, 8.10 and 6.29 days, respectively. This highlights the importance of accurate representation of hydraulic structures and the preference for 3D modelling in future studies. In particular, the results show that the operation of WSL, with momentum conservation, could improve the water renewal capacity in the water impoundment area by 64%. The concentration of tracer for the model without momentum adjustment also depicted high oscillations, which indicated that the tracer had limited mixing due to the smaller jets. This led to the accumulation of the channel water into the proximity of the openings and flushing the tracers towards the shoreline with limited mixing. Fig.16 illustrates the tracer distribution at the end of renewal time for each scenario. Higher concentrations were observed inside the lagoon near the coastline and particularly at the junction of the embankment with the coastline. This was due to the significant reduction in the velocity in these regions as a result of the structure, as observed in Fig.13. The concentration outside and to the east of WSL had also increased due to reductions in the local velocity as a result of the lagoon, i.e. Fig.13, and the sheltering effect of the lagoon.

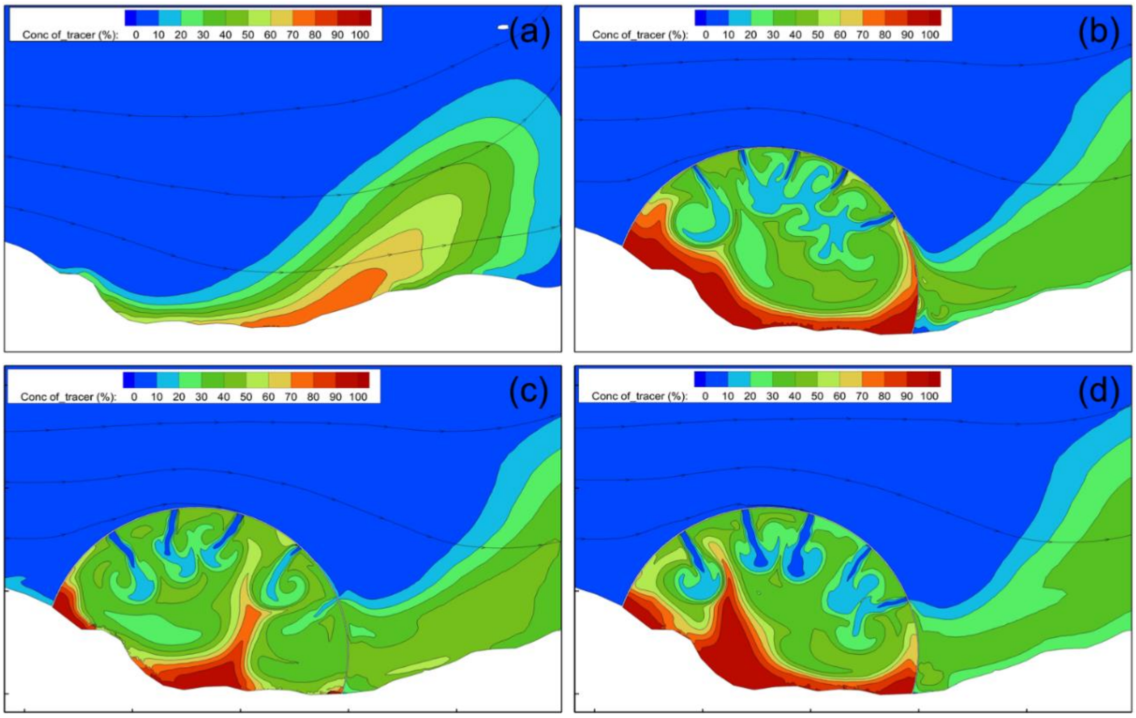

Fig. 14. Instantaneous tracer flushing distribution after 21.7 hours of release: (a) without lagoon; (b) with lagoon and mass balance only; (c) with lagoon and momentum using realistic source; (d) with lagoon and momentum using simplified source.

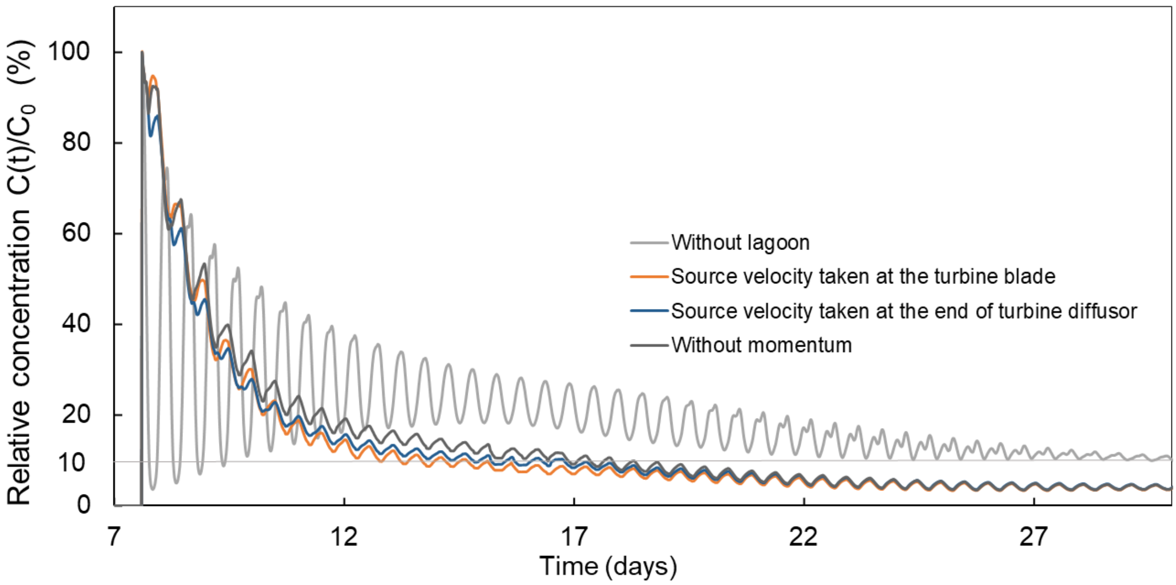

Fig. 15. Concentration variations of tracer in the initial release area for pre-WSL, and post-WSL with different momentum term settings.

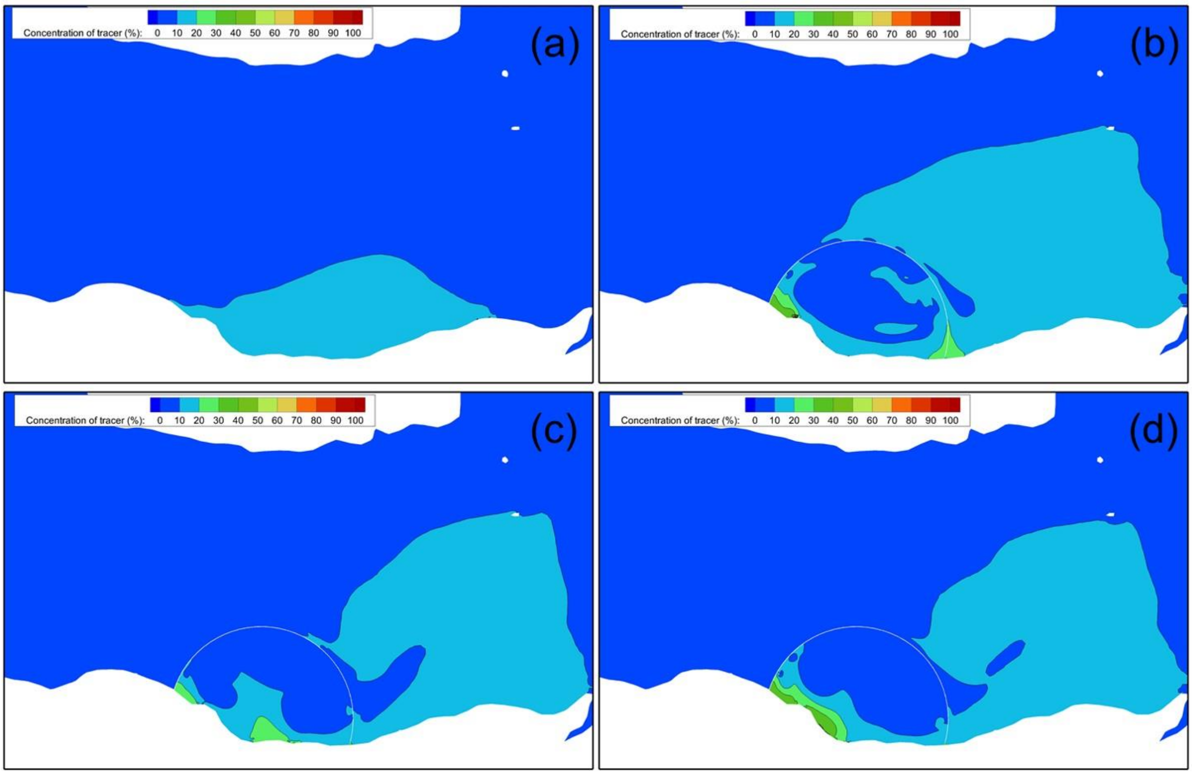

Fig. 16. Instantaneous tracer flushing distribution at the end of renewal time: (a) without lagoon; (b) with lagoon and mass balance only; (c) with lagoon and momentum using realistic source; (d) with lagoon and momentum using simplified source.

4.6 Bed shear stresses

The variations in both the maximum and averaged bed shear stresses for the pre- and post-lagoon configurations are shown in Fig. 17. The main changes are limited to the vicinity of the lagoon location and the inner Bristol Channel, following the similar changes observed for the velocity patterns. The peak increase in the maximum bed shear stress occurs in the lee of the turbine and sluice gate wakes, with the peak increase reaching 10-20 Pa, while outside of WSL there is a relatively large area identified where there is a slight increase in the bed shear stresses. This indicates that there is potential for scour and erosion in these areas as a result of the increased maximum bed shear stresses. Both the maximum and averaged bed shear stresses show a slight decrease inside the middle part of WSL. This decrease is mainly limited to 1-2 Pa. This decrease in the bed shear stresses indicates that sedimentation is more likely to occur in these regions inside WSL. This is a common problem for most tidal structures and needs to be carefully considered in any future design studies [19, 61, 68, 69].

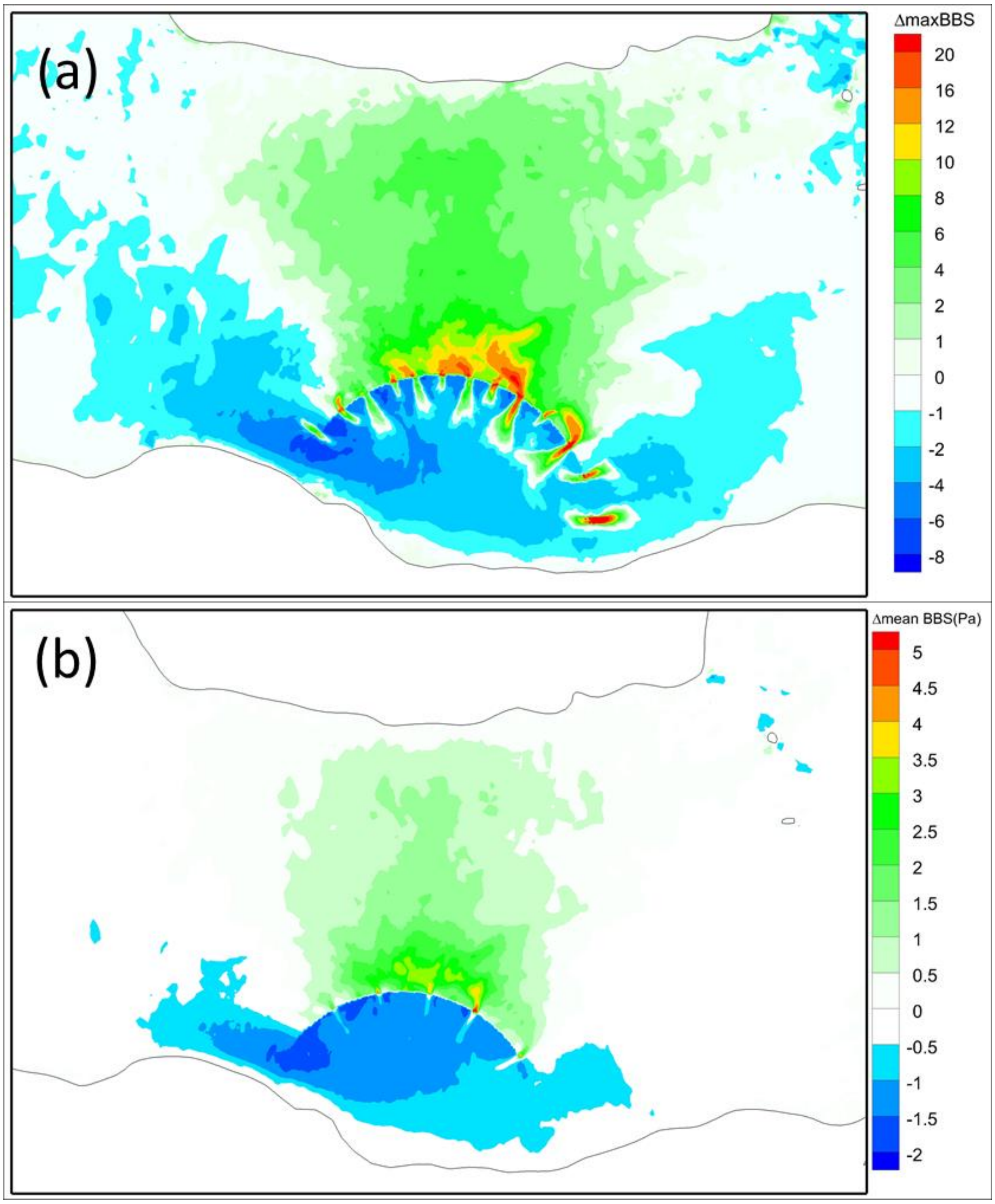

Fig. 17. Difference between the pre- and post-lagoon (a) maximum and (b) average bed shear stresses in the region around WSL.

The changes in the tidal velocities and the bed shear stresses are likely to have an impact on the morphological characteristics and the benthic environment, particularly in the region both within and around WSL. Previous field investigations have shown that the bed material in the region of WSL is primarily gravel, while much of the inner Bristol Channel tends to be more sand and bedrock [15, 70]. The decrease in the velocity field and bed shear stress distribution within and around WSL is therefore likely to lead to an accumulation of suspended sediments through deposition, which could, in turn, increase the risk of sedimentation. Moreover, sediment accumulation could threaten the survival of some benthic species [71, 72].

5 Conclusion

A high-resolution depth-averaged hydrodynamic model, namely TELEMAC-2D, has been used to model a proposed new tidal range energy generating lagoon, to be built in the Bristol Channel, namely the West Somerset Lagoon (WSL). WSL will have a maximum capacity of 2.5 GW, which would make this scheme one of the largest proposed lagoons to be built in the UK. The preliminary hydrodynamic and hydro-environmental impacts of the operation of WSL, and the impacts of different optimised operational strategies for the scheme, were investigated in this paper. The TELEMAC-2D model was refined to incorporate the hydraulic structures, namely turbines and sluice gates, using a fully conservative momentum formulation which included additional source terms, and with each component being operated independently. As a result of these refinements, the fully conservative scheme performed with encouraging results and showed less than 1% difference with the maximum annual energy generation predicted using an optimisation model.

The WSL was found to have various impacts on the hydrodynamics within the Bristol Channel and Severn Estuary including, in particular, increasing the amplitude of the M2, N2, S2 tidal constituents while increasing the phase on the western side of the lagoon and decreasing it to the east. Furthermore, the operation of WSL would generally increase the low-water levels and decrease the high-water levels in the Bristol Channel and Severn Estuary. The reduction in the high water levels would decrease coastal flood risk, and the increase in the low water levels would slightly benefit port access to shipping and recreational yachting in the shallow waters of the Severn Estuary. However, changes to the tidal range would also result in some loss in the area of the low intertidal mudflats, towards the head of the estuary, which might affect the biodiversity and feeding grounds for birds unless topographic raising were to be undertaken. These findings need further investigation in the future to enable the impacts to be determined more precisely, and particularly identifying the key sites of any changes within the estuary.

Except for the noticeable increase in the near-field maximum velocities in the turbine and sluice gate wakes, the maximum velocity in the inner Bristol Channel was predicted to increase by 0.25 to 0.75 m/s, while the corresponding maximum velocity decreased inside the lagoon, and across most of the plan-surface area away from the turbine and sluice gate wakes. The bed shear stress is related to the square of the velocity and therefore showed similar patterns of change as the velocity variations. The maximum bed shear stresses were predicted to increase by up to 20 Pa in the wake of the turbines and to decrease by 0.5-2.0 Pa across most of the lagoon. The renewal time was then predicted to assess the general flushing characteristics in the region. The conservative momentum formulation model, with the additional source term, indicated an decrease in the renewal time of 17% compared with the renewal time for a mass balance only model. This suggests that the higher velocities of the turbine and sluice gate wakes would benefit pollution transportation inside the lagoon, which would be meaningful in future design of TRSs of similar shapes and where there are potential pollution risks. These results indicated that the operation of the lagoon would decrease the renewal time from 22.4 days to 8.10 days for the pre-lagoon and post-lagoon cases respectively, and with the source term included. This demonstrates that WSL could improve the renewal time and flushing characteristics in the water impoundment area by 64% overall.

In summary, the study reported herein has shown that the West Somerset Lagoon offers a potentially attractive scheme for generating a significant level of tidal renewable energy, in an estuarine basin with a particularly large tidal range, and with the scheme having some positive and negative impacts on the flooding and environmental characteristics of the basin, but these are relatively small compared to the impacts of previous schemes studied in this basin. However, further research is required to provide more accurate information on the operational design of the scheme. This includes 3D modelling of the scheme, in order to more accurately understand the hydro-environmental and ecological impacts of the scheme.

6 Acknowledgements

The authors were supported by the Chinese Scholarship Council (CSC No.201606300064) and the EERES4WATER (Promoting Energy-Water nexus resource efficiency through renewable energy and energy efficiency) project, which is co-financed by the Interreg Atlantic Area Programme through the European Regional Development Fund, under EAPA 1058/2018. The authors are grateful for this support. The authors would also like to express their gratitude to Prof Chris Binnie and Mr David Kerr (Directors of TEES) for their extensive experience and instructive suggestion for providing the proposed layout and other information for the WSL scheme and generally for their helpful suggestions.

7 References

[1] Krohn D, Woods M, Adams J, Valpy B, Jones F, Gardner P. Wave and tidal energy in the UK. Tech Report, Renewable UK; 2013.
[2] Kadiri M, Ahmadian R, Bockelmann-Evas B, Rauen W, Falconer RA. A review of the potential water quality impacts of tidal renewable energy systems, Renew Sustain Energy Rev 2012;16(1):329-341.
[3] Waters S, Aggidis G. Tidal range technologies and state of the art in the review. Renew Sustain Energy Rev 2016;59:514-529.
[4] Cornett A, Cousineau J, Nistor I. Assessment of hydrodynamic impacts from tidal power lagoons in the Bay of Fundy. Int J Mar Energy 2013;1:33-54.
[5] Angeloudis A, Falconer RA. The sensitivity of tidal lagoon and barrage hydrodynamic impacts and energy outputs to operational characteristics. Renew Energy 2017;114(A):337-351.
[6] Hendry C. The role of tidal lagoons, Tech Report, UK Government, 2017.
[7] Twidell J, Weir T. Renewable energy resources. 2nd ed. Taylor & Francis; 2006.
[8] Waters S, Aggidis G. A World First: Swansea Bay Tidal lagoon in review. Renew Sustain Energy Rev 2016;56:916-921.
[9] Neill SP, Angeloudis A, Robins PE, Walkington I, Ward SL, Masters I, et al. Tidal range energy resource and optimization past perspectives and future challenges. Renew Energy 2018;127:763-778.
[10] Ahmadian R, Falconer RA, Lin B. Hydro-environmental modelling of the proposed Severn barrage, UK. P I Civil Eng-Energy 2010;163(3):107-117.
[11] Angeloudis A, Kramer SC, Hawkins N, Piggott MD. On the potential of linked-basin tidal power plants: an operational and coastal modelling assessment. Renew Energy 2020;155:876-888.
[12] Ashley M. Ecosystem service mapping in the Severn estuary and inner Bristol Channel. Report for NERC Marine Renewable Energy Knowledge Exchange Project, Plymouth; 2014.

[13] Elliott K, Smith HC, Moore F, van der Weijde AH, Lazakis I. Environmental interactions of tidal lagoons: A comparison of industry perspectives. Renew Energy 2018;119:309-319.
[14] Ahmadian R, Olbert AI, Hartnett M, Falconer RA. Sea level rise in the Severn Estuary and Bristol Channel and impacts of a Severn Barrage. Comput Geosci 2014;66:94-105.
[15] Kirby R. Distribution, transport and exchanges of fine sediment, with tidal power implications: Severn Estuary, UK. Mar Pollut Bull 2010;61(1-3):21-36.
[16] Adcock TAA, Draper S, Nishino T. Tidal power generation - a review of hydrodynamic modelling. Proc Inst Mech Eng Part a J Power Energy 2015;0(0):1-17.
[17] Gao G, Falconer RA, Lin B. Modeling effects of a tidal barrage on water quality indicator distribution in the Severn Estuary. Front Env Sci Eng 2013;7:211-218.
[18] Ahmadian R, Falconer RA, Bockelmann-Evans B. Comparison of hydro-environmental impacts for ebb-only and two-way generation for a Severn Barrage. Comput Geosci 2014;71:11-19.
[19] Xia J, Falconer RA, Lin B. Impact of different tidal renewable energy projects on the hydrodynamic processes in the Severn Estuary, UK. Ocean Model 2010;32:86-104.
[20] Kadiri M, Ahmadian R, Bockelmann-Evans B, Falconer RA, Kay D. An assessment of the impacts of a tidal renewable energy scheme on the eutrophication potential of the Severn Estuary, UK. Comput Geosci 2014;71(1):3-10.
[21] Kim JW, Ha HK, Woo SB. Dynamics of sediment disturbance by periodic artificial discharges from the world's largest tidal power plant. Estuar Coast Shelf Sci 2017;190:69-79.
[22] Evans P. Impacts of a Tidal Lagoon on Urban Drainage and Pollutant Dispersion in a Coastal Embayment. The 12th European Wave and Tidal Energy Conference (EWTEC), Cork, 2017;1144:1-10.
[23] Ahmadian R, Morris C, Falconer RA. Hydro-environmental modelling of off-shore and coastally attached impoundments off the north wales coast. In: Proceedings of the 1st European IAHR congress, Edinburgh;2010.
[24] Matta E, Koch H, Selge F, Simshäuser MN, Rossiter K, da Silva GMN, et al. Modeling the impacts of climate extremes and multiple water uses to support water management in the Icó-Mandantes Bay, Northeast Brazil. J Water Clim Change 2018;10(4),893-906.
[25] Monsen NE, Cloern JE, Lucas LV, Monismith SG. A comment on the use of flushing time, residence time, and age as transport time scales. Limnol. Oceanogr 2002;47:1545-1553.
[26] Xia J, Falconer RA, Lin B. Hydrodynamic impact of a tidal barrage in the Severn Estuary, UK. Renew Energy 2010;35:1455-1468.
[27] Angeloudis A, Falconer RA, Bray S, Ahmadian R. Representation and operation of tidal energy impoundments in a coastal hydrodynamic model. Renew Energy 2016;99:1103-1115.
[28] Čož N, Ahmadian R, Falconer RA. Implementation of a full momentum conservative approach in modelling flow through tidal structures. Water 2019;11(9):1917.
[29] Sanders BF. Non-reflecting boundary flux function for finite volume shallow water models. Adv Water Resour 2002;25:195-202.
[30] Xue J, Ahmadian R, Jones O, Falconer RA. Design of tidal range energy generation schemes using a Genetic Algorithm model. Appl Energy 2021;286:116506.
[31] Tidal Engineering and Environmental Services ltd. West Somerset Lagoon; 2020. https://tidalengineering.co.uk/west-somerset-lagoon/
[32] Xue J, Ahmadian R, Falconer RA. Optimising the operation of tidal range schemes. Energies 2019;12(15):2870.
[33] Baker AC. Tidal power. Proc Instit Electr Eng 1987;134(5):392-398.
[34] Jeffcoate P, Stansby PK, Apsley D. Near-field flow downstream of a barrage: experiments, 3-D, CFD and depth-averaged modelling. Proceedings of the 30th International Conference on Ocean, Offshore and Arctic Engineering, Rotterdam, The Netherlands, 2011; 909-18.
[35] Wang T, Yang Z, Copping A. A modeling study of the potential water quality impacts from in-stream tidal energy extraction. Estuaries Coasts 2015;38:173-186.
[36] Yang Z, Wang T. Effects of tidal stream energy extraction on water exchange and transport timescales. In: Yang Z, Copping A, editors. Marine renewable energy; 2017;259-278.
[37] Uncles R, Radford P. Seasonal and spring-neap tidal dependence of axial dispersion coefficients in the Severn-a wide, vertically mixed estuary. J Fluid Mech 1980;98:703-726.
[38] King J, Ahmadian R, Falconer RA. Hydro-epidemiological modelling of bacterial transport and decay in nearshore coastal waters. Water Res 2021;196:117049.
[39] Bray S, Ahmadian R, Falconer RA. Impact of representation of hydraulic structures in modelling a Severn Barrage. Comput and Geosci 2016;89:96-106.
[40] Hervouet J. Hydrodynamics of free surface flows, modelling with the finite element method. Cambridge: Cambridge University Press; 2007.
[41] POL. Continental Shelf Model: Fine Grid (CS3 and CS3-3D), 2011.

[42] Ji ZG. Hydrodynamics and water quality: modeling rivers, lakes, and estuaries: John Wiley & Sons; 2017.
[43] Stapleton CM, Wyer MD, Kay D, Bradford M, Humphrey N, Wilkinson J, Lin B, et al. Fate and Transport of Particles in Estuaries - Volume IV: Numerical Modelling for Bathing Water Enterococci Estimation in the Severn Estuary. Environment Agency Science Report SC000002, 2007;1-138.
[44] Abu-Bakar A, Ahmadian R, Falconer RA. Modelling the transport and decay processes of microbial tracers in a macro-tidal estuary. Water Res 2017;123:802-824.
[45] Guo B, Ahmadian R, Evans P, Falconer RA. Studying the Wake of an Island in a Macro-tidal Estuary. Water 2020;12:1225.
[46] Falconer RA, Xia J, Lin B, Ahmadian R. The Severn Barrage and other tidal energy options: hydrodynamic and power output modelling. Sci China Ser E:Technol Sci 2009;52(11):3414-3424.
[47] Xia J, Falconer RA, Lin B. Impact of different operating modes for a Severn Barrage on the tidal power and flood inundation in the Severn Estuary, UK. Appl Energ 2010;87:2374-2391.
[48] Chen Y, Lin B, Lin J, Wang S. Effects of stream array configuration on tidal current energy extraction near an island. Comput Geosci 2015;77:20-28.
[49] Aggidis G, Feather O. Tidal range turbines and generation on the Solway firth. Renew Energy 2012;43:9-17.
[50] Zhou J, Pan S, Falconer RA. Optimization modelling of the impacts of a Severn Barrage for a two-way generation scheme using a Continental Shelf model. Renew Energy 2014;72:415-427.
[51] Ahmadian R, Falconer RA, Bockelmann-Evans B. Far-field modelling of the hydro-environmental impact of tidal stream turbines. Renew Energy 2012;38:107-116.
[52] Falconer RA, Guo B, Ahmadian R. Coastal Reservoirs and their Potential for Urban Regeneration and Renewable Energy Supply. In: Sitharam TG, Yang SQ, Falconer RA, Sivakumar M, Jones B, Kolathayar S, Sinpoh L, editors. Sustainable Water Resource Development Using Coastal Reservoirs. 2020; 143-172.
[53] Ahn SH, Xiao Y, Wang Z, Zhou X, Luo Y. Performance prediction of a prototype tidal power turbine by using a suitable numerical model. Renew Energy 2017;113:293-302.
[54] Wilhelm S, Balarac G, Métais O, Ségoufin C. Analysis of Head Losses in a Turbine Draft Tube by Means of 3D Unsteady Simulations. Flow Turbul Combust 2016;97:1255-1280.
[55] Guillou N, Thiébot J, Chapalain G. Turbines' effects on water renewal within a marine tidal stream energy site. Energy 2019;189:116113.
[56] Dabrowski T, Hartnett M, Olbert A. Determination of flushing characteristics of the Irish Sea: a spatial approach. Comput Geosci 2012;45:250-260.
[57] Gao G, Xia J, Falconer RA, Wang Y. Modelling Study of Transport Time Scales for a Hyper-Tidal Estuary. Water 2020;12:2434.
[58] Easton MC, An Assessment of Tidal Energy and the Environmental Response to Extraction at a Site in the Pentland Firth, PhD. Thesis, The University of Aberdeen, 2013.
[59] Brière C, Abadie S, Bretel P, Lang P. Assessment of TELEMAC system performances, a hydrodynamic case study of Anglet, France. Coast Eng 2007;54:345-356.
[60] Pawlowicz R, Beardsley B, Lentz S. Classical tidal harmonic analysis including error estimates in MATLAB using T_TIDE. Comput and Geosci 2002;28:929-937.
[61] Haverson D, Bacon J, Smith HC, Venugopal V, Xiao Q. Cumulative impact assessment of tidal stream energy extraction in the Irish Sea. Ocean Eng 2017;137:417-428.
[62] Robins PE, Neill SP, Lewis MJ, Ward SL. Characterising the spatial and temporal variability of the tidal-stream energy resource over the northwest European shelf seas. Appl Energy 2015;147:510-522.
[63] Burton NH, Musgrove AJ, Rehfisch MM, Clark NA. Birds of the Severn Estuary and Bristol Channel: their current status and key environmental issues. Mar Pollut Bull 2010;61:115-123.
[64] Clark NA. Tidal barrages and birds. Ibis 2006;148:152-157.
[65] Duggins DO, Dethier MN. Experimental studies of herbivory and algal competition in a low intertidal habitat. Oecologia 1985;67:183-191.
[66] Neill SP, Scourse JD. The formation of headland/island sandbanks. Cont Shelf Res 2009;29:2167-2177.
[67] Neill SP, Litt EJ, Couch SJ, Davies AG. The impact of tidal stream turbines on large-scale sediment ynamics. Renew Energy 2009;34:2803-2812.
[68] Carroll B, Li M, Pan S, Wolf J, Burrows R. Morphodynamic Impacts of a Tidal Barrage in the Mersey Estuary. World Scientific Publishing Company 2008;2743-2755.
[69] Wolf J, Walkington IA, Holt J, Burrows R. Environmental impacts of tidal power schemes. Proc ICE Maritime Eng 2009;162:165-177.
[70] Cannard P. The Sediment Regime of the Severn Estuary Literature Review. Tech Report; 2016.
[71] Rogers, CS. Responses of coral reefs and reef organisms to sedimentation. Mar Ecol Prog Ser 1990;62:185-202.
[72] Short FT, Wyllie-Echeverria S. Natural and human-induced disturbance of seagrasses. Environ Conserv 1996; 23:17-27.